JCTC Journal of Chemical Theory and Computation

Article

pubs.acs.org/JCTC

Aspects of Size-Consistency of Orbitally Noninvariant Size-Extensive Multireference Perturbation Theories: A Case Study Using UGA-SSMRPT2 as a Prototype

Avijit Sen, Sangita Sen, and Debashis Mukherjee*

Raman Center for Atomic, Molecular and Optical Sciences, Indian Association for the Cultivation of Science, Kolkata 700 032, India

ABSTRACT: Profiling a potential energy surface (PES), all the way to dissociate a molecular state into particular fragments and to display real or avoided crossings, requires a multireference description and the maintenance of size-consistency. The many body methods, which suit this purpose, should thus be size-extensive. Size-extensive theories, which are invariant with respect to transformation among active orbitals are, in principle, size-consistent. Relatively cheaper size-extensive theories, which do not possess this invariance, can still be size-consistent if the active orbitals are localized on the asymptotic fragments. Such methods, if perturbative in nature, require the use of an unperturbed Hamiltonian, which has orbital invariance with respect to the transformation within active, core, and virtual orbitals. The principal focus of this paper is to numerically realize size-consistency with localized active orbitals using our recently developed orbitally noninvariant Unitary Group Adapted State Specific Multireference second order Perturbation Theory (UGA-SSMRPT2) as a prototype method. Our findings expose certain generic potential pitfalls of size-extensive but orbitally noninvariant MRPT theories, which are mostly related to the inability of reaching proper localized active orbitals in the fragments due to the artifacts of the orbital generation procedure. Despite the invariance of the zeroth order CAS function, lack of invariance of the MRPT itself then leads to size-inconsistency. In particular, reaching symmetry broken fragment active orbitals is an issue of concern where suitable state-averaging might ameliorate the problem, but then one has to abandon full orbital optimization. Additionally, there can be situations where the orbitals of the fragment reached as an asymptote of the supermolecule are not the same as those obtained from the optimization of the fragments individually and will require additional transformation. Moreover, for a certain PES, one may either abandon the use of optimized orbitals for that state to preserve proper symmetry and degeneracy in the fragment orbitals or be satisfied with the use of optimized orbitals, which generate broken symmetric orbitals in the fragmentation limit. All these pathologies are illustrated using the PES of various electronic states of multiply bonded systems like N_2, C_2H_2, HCN, C_2, and O_2. Subject to such proviso, the UGA-SSMRPT2 turns out to be an excellent theory for studying the PES leading to fragmentation of strongly correlated systems satisfying the requirements of size-consistency with localized active orbitals. An unexpected spin-off of our studies is the realization that the size-inextensive MRMP2, which bears a close structural similarity with our theory, might under certain situations display size-consistency. We analyze this feature concretely in our paper. Our studies may serve as a benchmark for monitoring numerically the size-consistency of any state specific multireference theory which is size-extensive but not invariant with respect to transformation of active orbitals.

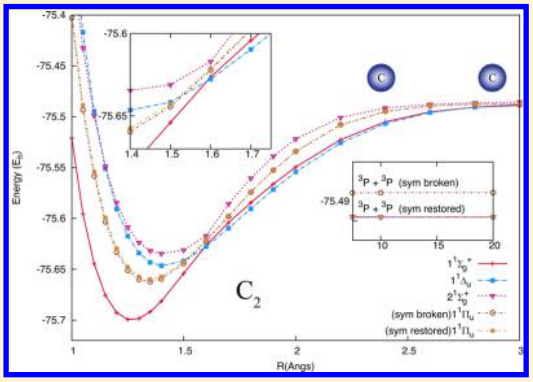

INTRODUCTION

Accurate computation of potential energy surfaces (PES) continues to be a fertile research frontier as it brings forth the field of quantum chemistry as providing a reliable tool for prediction of reaction pathways, catalysts, spectroscopic signatures, and myriad other possible phenomena. The potential energy profile of a molecule is the outcome of an interplay of a large number of physical interactions which can be conveniently and operationally separated into a hierarchy of correlated descriptions beyond a "mean field" model. To take care of the quasi-degeneracy of some orbitals at various geometries, which are responsible for real and avoided curve crossings and to provide the required flexibility to describe the fragment molecular states in the limit of asymptotic separation into fragments in various channels, the mean field description warrants the use of a multiconfiguration wave function as a starting point where the components of these functions display varying degrees of quasi-degeneracy with respect to changes in nuclear geometry. The correlation energy captured in this mean field function is usually known as nondynamical correlation. The correlation brought out by the interaction of the virtual functions obtained by excitation of electrons from the mean field function provides the so-called dynamical correlation. These two correlation effects are coupled, wherein lies the necessity of modeling these two contributions in a balanced manner. While nondynamical correlation turns out to be strong, requiring diagonalization in the space of quasi-degenerate components of the starting

Received: May 17, 2015
Published: July 20, 2015

DOI: 10.1021/acs.jctc.5b00457
J. Chem. Theory Comput. 2015, 11, 4129−4145

functions, the dynamical correlation comes out as contributions from a large number of virtual functions whose collective effect requires formalisms, which scale properly with respect to both the system size and to conform with the requirement of providing the correct fragmentation limit. In the well-known many body terminology, the property of the correct scaling of energy with respect to the system size (essentially with respect to the number of electrons) is called size-extensivity,[1−5] while the property of generating the asymptotic energy as a sum of fragments energies obtained with the same method is called size-consistency.[6] Though it is often possible to prove size-extensivity analytically, for some theories, it may be quite demanding, and in such cases, well-defined procedures have been suggested by Mukherjee et al.[7] to discern size-extensivity or otherwise numerically. Such analyses are now known as generalized extensivity.

Single reference (SR) theories capture dynamical correlation effectively in the absence of quasi-degeneracy. However, no SR description at the mean field level usually satisfies size-consistency and is therefore not a natural starting point for theories for computing PES. They may be, however, size-extensive when formulated in the perturbative and CC framework, as in SR Möller-Plesset (MP)[8] perturbation theory at various orders and the single-reference coupled cluster theory (SRCC).[2,6,9] These are intrinsically superior to the algebraically much simpler SR configuration interaction (CI)[10] method, which is size-inconsistent. To capture nondynamical correlations with proper scaling, any good theory for PES must be built around some version or other of multireference PT or CC (to be henceforth called MRPT or MRCC), rather than an MRCI.[11]

Most multireference many body theories are based on the concept of an active space spanned by a set of "model functions" (ϕ_μ), which, if complete (ie. a CAS), with respect to a set of potentially degenerate orbitals (called "active orbitals"), ensures size-extensivity and size-consistency of the corresponding energy at the zeroth order description. But, maintaining size-extensivity and size-consistency after incorporation of the dynamical correlation is much harder to accomplish. The doubly occupied core and the empty virtual orbitals in the CAS are generically called "inactive orbitals", at least one of which has to be involved to contribute to the dynamical correlation energy.

The development of size-extensive and size-consistent MRPT and MRCC theories, based on the multireference description of the starting function, are neither unique nor straightforward. There are various formalisms of varying degrees of sophistication and they emphasize different aspects of correlation and of the ease of computation. Historically, the oldest MR many-body formalisms were based on the concept of effective Hamiltonians,[12−14] defined on a CAS where a single wave operator, Ω, is used to convert the N starting combinations of the model functions for the N roots. One major deterrent in a smooth implementation of an MRPT/MRCC with effective Hamiltonians defined in a CAS is the numerical instability arising out of the problem of intruder states[15,16] since it is virtually impossible to find an N-dimensional CAS which provides a good qualitative description of all the N exact roots throughout a full PES, even when the theories used are size-extensive and size-consistent.

The MRCCs based on effective Hamiltonians are of different types, often classified as the Valence-Universal (VUMRCC)[17,18] and the State-Universal (SUMRCC)[19] theories. They have been widely used, mostly to describe energy differences of spectroscopic interest (with VUMRCC) or for computing energies of multireference states (with SUMRCC), but usually they are not very successful for generating PES (though several studies have been made with VUMRCC, often needing switching to different active spaces at different geometries[20−23]). The PT counterparts of the corresponding MRCCs such as valence universal multireference perturbation theory (VUMRPT) from valence universal multireference coupled cluster theory (VUMRCC),[17,18] a possible state universal multireference perturbation theory (SUMRPT) from the state universal multireference coupled cluster theory (SUMRCC or UGA-SUMRCC),[19,24] and multiconfiguration quasi-degenerate perturbation theory (MCQDPT2),[25−27] which is a multiroot generalization of MRMP2,[28,29] are all based on effective Hamiltonians.

To bypass the problem of intruders, it was felt necessary to abandon the familiar effective Hamiltonian formalisms. There are essentially three major developments in this regard:

(i) To work with an incomplete active space (IAS)[30−33] by leaving out the higher lying portion of the CAS, which is energetically close to the low-lying portion of the virtual space. However, ensuring size-extensivity requires abandoning the traditional choice of the intermediate normalization of the wave operator.[30−32] There have been numerous applications of such theories, both in the VUMRCC and the SUMRCC setting,[22,34] but again PES studies have not been that numerous.

(ii) To use the approach of intermediate Hamiltonians[35−43] where one imposes a weaker condition that only certain M (M < N) roots of the effective operator are the eigenvalues of H.

(iii) One may also envisage the extreme variant of the intermediate Hamiltonian where only one root is targeted (i.e., M = 1). This is the state specific multireference approach,[44−46] where one may adopt either a contracted MR starting function or a decontracted one. In the contracted versions, the combining coefficients of the functions of the active space are precomputed and kept frozen when a wave operator introduces dynamical correlation. In the decontracted versions, one can relax the combining coefficients as a result of coupling of the nondynamical and dynamical correlations. The internally contracted MRCC (icMRCC) theories[45,47−51] are of the contracted variety, while others such as those of Malrieu et al.,[52] BW-MRCC,[53,54] MkMRCC,[45,46] and the most recent UGA-SSMRCC[55] are of the uncontracted variety. Similarly, contracted PTs such as the CASPT[56−59] and the original formulation of NEVPT2,[60,61] uncontracted PTs like MRMP2,[28,29] MROPT[62], SSMRPT,[63−65] MkMRPT,[66] and the spin adapted SSMRPT analogues, SA-SSMRPT[67,68] and UGA-SSMRPT2,[69] belong to the decontracted category.

Of the three approaches mentioned above, the intermediate Hamiltonian and state specific formalisms seem to be very promising. Equation of motion approaches built on an MR starting functions, although not fully size-extensive, provide access to both multiroot and single root formalisms.[70−74] The developments over the last three decades have amply demonstrated that while suitable MRCC formalisms are intrinsically more accurate,[24,45−49,51,53−55,75,76] for large systems, development and implementations of size-extensive MRPT formulations would continue to be of considerable importance for their lower computational demands. In particular, certain

DOI: 10.1021/acs.jctc.5b00457
J. Chem. Theory Comput. 2015, 11, 4129−4145

formulations of MRPTs following approaches (ii) and (iii) offer the possibility of predicting the nature of the PES preserving the essential profile quite faithfully.[28,29,57,67−69,77] It should be mentioned here that NEVPT2, originally suggested by Malrieu[60,78] (see also ref 61) has the flexibility in that it can, in principle, be formulated in a hybrid way to encompass both the effective Hamiltonian and the intermediate Hamiltonian and also in a contracted and partially decontracted manner (see, e.g., ref 61). There are also other very interesting formulations like Generalized Van-Vleck PT (GVVPT),[79−81] Multi-Configuration PT (MCPT),[82−84] APSG based PT,[85,86] block-correlated PT,[87] and the so-called Static-Dynamic-Static (SDS) PT.[88]

It should be noted at this point that several of the state-specific PT or CC theories are unfortunately not size-extensive. An equally important concern for us is that several of the size-extensive formulations are not invariant with respect to orbital transformations within each class. While the extant invariant size-extensive state-specific multireference methods[47,48,50,60] satisfy all the desired requirements discussed above, they are necessarily somewhat expensive. Here, the noninvariant size-extensive method offers real computational advantages[37,39,45,46,55,63−69] since they can be easily used to explore the fragmentation processes in the PES profile via the use of localized orbitals.

In this paper, we will look at the various aspects of numerically realizing size-consistency of a particular version of a noninvariant state specific MRPT, viz., the recently developed spin-free UGA-SSMRPT2,[69] which emanates as a perturbative approaximant to the UGA-SSMRCC.[55] We, therefore, would not dwell on variants (i)−(iii) of the MRCC any further, unless they are relevant for this paper. We instead quote here pertinent references for comprehensive reviews on the recent developments of the various MRCCs.[4,89−93] We choose UGA-SSMRPT2 as a prototype for a size-extensive noninvariant MRPT theory because in our opinion it is structurally the simplest perturbation theory which is rigorously size-extensive and is also spin-free. Since it is noninvariant with respect to transformation among active orbitals, localized active orbitals have to be used to study size-consistency numerically. We emphasize here, though, that the issues discussed in this paper are generic for any size-extensive noninvariant formalism.

The paper is organized as follows: In the section on UGA-SSMRPT2, we give a brief recapitulation along with its analytic proof of size-extensivity and a more detailed analytical demonstration of its size-consistency. The section titled Issues Related to Size-Consistency in UGA-SSMRPT2 and Related MRPTs forms the central part of the paper, wherein discussions of issues relating to its size-consistency and orbital dependence are presented. The three inter-related issues, which have to be considered as we proceed, are (a) the implication of the invariance of the reference functions with respect to orbital transformation within each class, (b) the necessity of choosing an unperturbed Hamiltonian H_0, which displays the invariance with respect to such transformations, and (c) the consequences of such choices in ensuring size-consistency by an analysis of the restricted invariance of the working equations determining the perturbative cluster amplitudes. Moreover, we will have to resolve the tricky issue of ensuring full compatibility of the fragment active orbitals and the corresponding orbitals of the fragments as are obtained for the supermolecule in the fragmentation limit. Such congruence is essential for ensuring size-consistency, and appropriate orbital transformation may be called for. Related observations were noted by some earlier researchers[94] in the N−N bond breaking processes of N_2O_2. We have encountered in our numerical studies the surprising and unanticipated result that the widely used noninvariant and size-inconsistent MRPT, the MRMP2[29] theory, which is structurally close to our UGA-SSMRPT2, shows size-consistency in certain fragmentation limits of specific molecular states. We have analyzed carefully in the subsection titled An Aside: "Accidental" Size-Consistency of MRMP2 in Certain Situations, as an interlude, the conditions under which MRMP2 will be size consistent. The section titles Numerical Investigation of Size-Consistency of Multiply Bonded Molecules presents the application of UGA-SSMRPT2 to compute the PES of several electronic states of N_2, C_2H_2, and HCN, which form a set of triply bonded isoelectronic molecules but show varied characteristics in their PES along with more complicated molecules like C_2 and O_2 to investigate the size-consistency for different fragment limits. A comparative study of size-consistency is also undertaken vis a vis MRMP2 as a verification of our theoretical analysis. In the section titled Summary and Concluding Remarks, we summarize our findings and show their general applicability to related theories.

UGA-SSMRPT2

Many multireference perturbation theories to date have been developed from physical considerations. However, it is always possible to develop a perturbative analogue of a multireference coupled cluster theory preserving all the essential features of the corresponding MRCC. The only additional innovation required is to select a physically motivated zeroth order Hamiltonian, H_0, such that the perturbative approximation is valid and all the important physics incorporated. It is an interesting feature of any second order perturbation theory for energy that the diagonal part of the zeroth order Hamiltonian may be altered at will without affecting the matrix element connecting a virtual function with a model function via the perturbation (V) since the diagonal part of the perturbation does not contribute to the first order wave function. There are both advantages and disadvantages stemming from this property of the second order energy: while flexibility is gained, the uniqueness of the H_0 is lost. Moreover, when the reference function is multireference, the partitioning of H_0 may be either universal or different for each model function. The latter was first suggested by Zaitsevskii and Malrieu[95] and is called "multipartitioning". In our UGA-SSMRPT2, we adopt the latter class of partitioning.

Our UGA-SSMRPT2 is based on the linearized version of the parent spin-free UGA-SSMRCC.[55] The UGA-SSMRCC uses a normal-ordered multiexponential Ansatz for the component of the wave operator, Ω_μ,

$$\Omega = \sum_\mu \Omega_\mu = \sum_\mu \{e^{T_\mu}\}|\phi_\mu\rangle\langle\phi_\mu| \tag{1}$$

acting on the spin-adapted configuration state functions (CSF), $\{\phi_\mu\}$, comprising the CAS function $\Psi_0 = \Sigma_\mu|\phi_\mu\rangle c_\mu^{(0)}$, akin to the Jeziorski−Monkhorst (JM) Ansatz.[19] The operator parts of the T_μs are defined in terms of the generators of the unitary group. The normal ordering denoted by {...} is with respect to the common closed shell part of all the CSFs, in order to have a spin-adapted wave function even with a nonlinear wave operator Ansatz. *This is where we depart from the original Jeziorski−Monkhorst Ansatz.* The normal ordering was invoked to prevent contractions among the various T_μs in Ω_μ. Such contractions are unwanted since this would lead to nonterminating series in the cluster amplitudes. An ordinary exponential Ansatz of Ω_μ would have entailed them, and this is the principal reason why the

DOI: 10.1021/acs.jctc.5b00457
J. Chem. Theory Comput. 2015, 11, 4129−4145

earlier unitary group based coupled cluster theories[96,97] are not easily amenable to general implementation and application to increasing levels of sophistication of the theory and handling of arbitrary active spaces. The normal ordering introduced in UGA-SSMRCC leads to the necessity for somewhat different algebraic manipulation than what are adopted in the spinorbital-based SSMRCC[45,46] (also known as MkMRCC[98]) developed earlier. For detailed discussions on the various aspects of the UGA-SSMRCC theory, we refer to our recent exhaustive papers.[55,93]

We now recapitulate briefly only the salient features of the development, referring to our very recent UGA-SSMRPT2 paper for the details.[69] Using any partitioning of the Hamiltonian, $H = H_0 + V$ and considering the amplitudes of the T_μs to be of first order, the first order perturbative approximation to the UGA-SSMRCC is given by

$$\langle\chi_\mu^l|H|\phi_\mu\rangle c_\mu^0 + \langle\chi_\mu^l|\{\overbrace{H_0T_\mu^{(1)}}\}|\phi_\mu\rangle c_\mu^0 - \sum_\nu \langle\chi_\mu^l|\{\overbrace{T_\mu^{(1)}W_{\nu\mu}}\}|\phi_\mu\rangle c_\mu^0 + \sum_\nu \langle\chi_\mu^l|\{T_\nu^{(1)} - T_\mu^{(1)}\}|\phi_\mu\rangle H_{\mu\nu}c_\nu^0 = 0 \quad (2)$$

$W_{\nu\mu}$ is the closed part of the operator $H + \overbrace{H_0T_\mu}$ interconverting the configuration state function (CSF) ϕ_μ to ϕ_ν. The relaxed second order energy $E_r^{[2]}$ is obtained as an expectation value, $E_{ur}^{[2]}$:

$$\sum_\nu \tilde{H}_{\mu\nu}^{[2]}c_\nu' = E_r^{[2]}c_\mu' \quad (3)$$

The relaxed coefficients, c_μ', emerge as the parameters of the perturbed wave function. The unrelaxed energy, $E_{ur}^{[2]}$, similarly is given by

$$\sum_{\mu\nu} c_\mu^{(0)}\tilde{H}_{\mu\nu}^{[2]}c_\nu^{(0)} = E_{ur}^{[2]} \quad (4)$$

where

$$\tilde{H}_{\mu\nu}^{[2]} = \langle\phi_\mu|\bar{H}_\nu|\phi_\nu\rangle = H_{\mu\nu} + \sum_l H_{\mu l}t_\nu^{l^{(1)}} \quad (5)$$

$\tilde{H}^{[2]}$ is the effective operator providing the appropriate second order energy, as given by eqs 3 and 4.

We depart from the CC analogue (viz., the UGA-SSMRCC)[55] in our UGA-SSMRPT2 in two important aspects. First, the UGA-SSMRPT2 makes use of amplitude equations for determining the t-amplitudes as against the projection equations of UGA-SSMRCC advocated by Maitra et al.[55] Since the operator manifold is not fully linearly independent, these two approaches are inequivalent. The latter approach involves the use of reduced density matrices (RDMs) in the working equations making them more complicated and the proof of the connectivity of the t-amplitudes and the consequent size-extensivity of the theory more difficult. However, this has been achieved by Maitra et al.[99] The former approach, i.e., amplitude equations, affords the facility of converting the normal ordering of the T_μs for each model function, ϕ_μ, to a new normal ordering with respect to the largest closed shell part of ϕ_μ, $\phi_{0,\mu}$. This is a departure from the approach in UGA-SSMRCC where the normal ordering is done with respect to the common closed shell part of all the ϕ_μs but can be shown to be exactly equivalent.[67] This results in a reduction in the number of classes of T_μs to be handled. Moreover, since RDMs do not occur in the amplitude equations, the size-extensivity of the equations becomes pretty obvious. The use of amplitude equations to solve for the T_μs implies that we can use any set of operators to span the excitation space without concerning ourselves with their linear dependence as long as the operators which are proportional to each other are not superfluously included. We take care to remove higher rank operators which are proportional to one of lower rank. It has been conclusively demonstrated by Szabados et al.[100] that these proportional operators play the largest role in destabilizing the solution of SSMRPT equations leading to erratic behavior of the PES, and we do not have these redundant operators in our cluster operators, T_μ.

An interesting feature to note is that our UGA-SSMRPT2 and the SA-SSMRPT of Mao et al.[67,68] (which is a spin-adapted PT analogue of the ordinary SSMRCC) differ in the structure of the equations, although the physical content is similar. The $[H_0,T_\mu]$ commutator of SA-SSMRPT is converted here to the second and third terms of eq 2. This affords the flexibility of choosing $W_{\nu\mu}$ as any closed part of the Hamiltonian, not necessarily H_0. However, when $W_{\nu\mu}$ is H_0, the equations become identical to that of SA-SSMRPT. We must mention here, as an aside, that the two formulations also differ in the choice of H_0: while SA-SSMRPT uses a diagonal H_0, our UGA-SSMRPT2 uses a "class diagonal" H_0. A "class-diagonal" H_0 can only induce scattering within each class of orbitals, viz., inactive core, active, and inactive virtual, keeping the formulation as close as possible to the Möller−Plesset partitioning in single reference theory. We have found that a normal ordering of the Hamiltonian with respect to $\phi_{0,\mu}$ naturally suggests a multipartitioning in H_0, where when acting on ϕ_μ it has the expression,

$$H_0{}_P^Q = \tilde{f}_\mu{}_P^Q = f_{0,\mu}{}_P^Q + \sum_{u_s\in\phi_\mu} (v_{Pu_s}^{Qu_s} - \delta_{P,u_s}v_{Pu_s}^{u_sQ})\gamma^{\mu\mu}{}_{u_s}^{u_s} \quad (6)$$

where,

$$f_{0,\mu}{}_P^Q = f_{c}{}_P^Q + \sum_{u_d\in\phi_{0,\mu}} [2v_{Pu_d}^{Qu_d} - v_{Pu_d}^{u_dQ}] \quad (7)$$

with P,Q denoting general orbital indices, and u_s and u_d denoting singly and doubly occupied active orbitals in ϕ_μ, respectively. The term involving δ_{Pu_s} takes care of the subtraction of the spurious interaction involving two electrons in u_s, when $P = u_s$. Equation 7 indicates that $f_{0,\mu}{}_P^Q$ is the matrix element of a Fock-like operator corresponding to the vacuum, $\phi_{0,\mu}$, and $\tilde{f}_\mu{}_P^Q$ is the corresponding quantity for ϕ_μ. $f_{c}{}_P^Q$ is the Fock operator for the common closed shell part of the model functions, identical to that used in UGA-SSMRCC.[55]

Use of $H_{\mu\nu}$ in the coupling term takes care of two important issues. First, it is responsible for the intruder-free nature of the UGA-SSMRPT2, and second, its dependence, on both ϕ_μ and ϕ_ν, is vital in establishing the connectivity of the working equations eventually leading to size-extensivity. The essential arguments have been presented in our earlier, more elaborate publication,[69] but for a more detailed analysis, we refer to the paper by Maitra et al.[55] However, the use of $H_{\mu\nu}$ in the coupling term makes it a second order term. Here, we abandon the order argument in favor of size-extensivity—an attitude we had advocated earlier also in the spinorbital based SSMRPT.[65] In this paper, it is more pertinent to underline the origin of size-consistency of UGA-SSMRPT2 with localized active orbitals. This we will undertake and analytically demonstrate below. We will also indicate where other allied theories differ in their structure from ours as regards maintaining rigorous size-consistency.

DOI: 10.1021/acs.jctc.5b00457
J. Chem. Theory Comput. 2015, 11, 4129−4145

The orbital noninvariance in any MRPT or MRCC theory, using the multiexponential JM Ansatz (or normal-ordered multiexponential Ansatz like in UGA-SSMRPT or UGA-MRCC) with respect to transformation of active orbitals arises from noninvariance of the correlated function in an approximate scheme as a consequence of the noninvariance of the model functions, ϕ_μ, under the transformation of active orbitals leading to the model function dependence of the cluster amplitudes of a T_μ. This an unavoidable problem with such types of Ansätze, which is why the active orbitals need to be localized on fragments for ensuring size-consistency. Localization ensures that provided the underlying mean field theory gives a size consistent wave function in the asymptotic limit each active orbital is entirely on one fragment. The size-extensivity of the theory then ensures in principle that the cluster amplitudes, T_μ, involve orbitals on one fragment only, and the wave function for the supermolecule is, hence, exactly a product of the corresponding approximate correlated wave functions of the fragments.

Let us assume that we are using localized active orbitals on fragments A and B and look at the expressions for cluster amplitudes from our UGA-SSMRPT2 with $W_{\nu\mu}$ taken as the $H_{0,\mu\nu}$. With the choice of a class-diagonal H_0, the nonvanishing term of W is of the form $W_{\nu\mu}$ when acting on ϕ_μ, and we can express $t^l_\mu(\mu)$ for UGA-SSMRPT2 in an alternate form as

$$t^l_\mu(\mu) = \frac{H^l_\mu + \{\overbrace{H_0 T_\mu}\}^l_\mu - \{\overbrace{T_\mu W_{\nu\mu}}\}^l_\mu}{E_{CAS} - H^0_{ll} + H^0_{\mu\mu} - H_{\mu\mu} - \sum_{\nu\neq\mu} \frac{t^l_\mu(\nu) H_{\mu\nu} c_\nu}{t^l_\mu(\mu) c_\mu}} \quad (8)$$

The terms entering eq 8 need some explanations. The (μ), (ν), etc. in the cluster amplitudes, t, indicate that the corresponding Ts occur in Ω_μ, Ω_ν, etc. The upper and lower indices on the operator T indicate that they are the amplitudes for the excitation from a model function labeled by the lower index to a virtual function labeled by the upper index. Specifically, an amplitude like $t^l_\mu(\nu)$ indicates that it belongs to the cluster operator T_ν, and the excitation operator accompanying t^l_μ would excite ϕ_μ to χ_l. The second and third terms in the numerator of the eq 8 are explicitly connected quantities.

In the fragmentation limit, both the full H and the unperturbed H_0 are additively separable into A and B. While it is obvious that the full H is invariant under transformations among the orbitals, a class-diagonal H_0 as used by us satisfies the invariance under transformations within the three classes of orbitals: core, active, and virtual only. The types of ts involved in the excitation of this fragmented system can basically be of three types: (a) **type 1**, where excitation is only on one fragment, (b) **type 2**, where there are cross-scatterings or transfer of electrons from A to B or vice versa, and (c) **type 3**, where there are simultaneous excitations on both the fragments. Our intention is to establish that in the asymptotic limit, the cluster amplitudes of types 2 and 3, T_{AB}, vanish, and those of type 1 involving excitation from one fragment only are independent of the other fragment.

Clearly, types 2 and 3 involve scattering from orbitals belonging to both A and B, and it is easy to show, using the extensivity of H and the class diagonality of H_0 and W, that these are zero in the fragmentation limit. To see this, consider any $t^{l\,AB}_{\mu\,AB}$ of type 2 or 3 corresponding to excitation/scattering from the composite $(\mu) \equiv (\mu_A\mu_B)$, where l_{AB} is the composite index involving orbitals A and B, with either a structure $t^{l_A\lambda_B}_{\mu_A\mu_B}(\mu_A\mu_B)\ \forall\ \lambda_B \neq \mu_B$ (for type 2) or $t^{l_A l_B}_{\mu_A\mu_B}(\mu_A\mu_B)$ (for type 3).

$$t^l_\mu(\mu_A\mu_B)^{AB}_{AB} = \frac{H^{l_{AB}}_{\mu_A\mu_B} + \{\overbrace{H_0 T_\mu}\}^{l_{AB}}_{\mu_A\mu_B} - \{\overbrace{T_\mu W_{\nu\mu}}\}^{l_{AB}}_{\mu_A\mu_B}}{E_{CAS} - H^0_{ll} + H^0_{\mu\mu} - H_{\mu\mu} - \sum_{\nu\neq\mu} \frac{t^l_\mu(\nu) H_{\mu\nu} c_\nu}{t^l_\mu(\mu) c_\mu}} \quad (9)$$

Since H_0 and W are class-diagonal, it follows that in the numerator of eq 9 determining $t^{l\,AB}_{\mu\,AB}(\mu_A\mu_B)$, only Ts of the same class can contribute. Since the first term of the numerator, viz., H, connecting $\mu_A\mu_B$ to l_{AB} involves orbitals belonging to both A and B, this term is zero by the extensivity of H. If we start by taking all the $t_{\mu A\mu B}$s in the second and third terms to be zero in the first iteration, the $t^{l_{AB}\,(1)}_{\mu_A\mu_B}$ is zero since the numerator is zero leading to all the T_{AB}s obtained from the first iteration being zero. In the second iteration, the excitation containing the Hamiltonian is zero, and so are the terms $\{\overbrace{H_0 T^{(1)}(\mu_A\mu_B)}\}^{l_{AB}}_{\mu_A\mu_B}$ and $\{\overbrace{T^{(1)}(\mu_A\nu_B) W}\}^{l_{AB}}_{\mu_A\mu_B}$, where $T^{(1)}(\mu_A\mu_B)$ are the appropriate components of $T^{(1)}_{AB}$ from the first iteration. Then all the $T^{(2)}_{AB}$s of the same class are zero by the same argument in the second and subsequently in all the successive iterations.

For the Ts of type 1, some more elaborate manipulations are needed. Let us assume for concreteness that we are computing the amplitude $t^{l_A}_{\mu_A}(\mu_A\ \nu_B)$. Its expression is given by

$$t^{l_A}_{\mu_A}(\mu_A\nu_B) = \frac{H^{l_A}_{\mu_A} + \{\overbrace{H_0 T_{AB}}\}^{l_A}_{\mu_A} - \{\overbrace{T_{AB} W}\}^{l_A}_{\mu_A}}{E_{CAS_A} + E_{CAS_B} - H^0_{l_A l_A} - H^0_{\nu_B\nu_B} + H^0_{\mu_A\mu_A} + H^0_{\nu_B\nu_B} - \sum_{\sigma_{AB}\neq\mu_A\nu_B} \frac{t^{l_A}_{\mu_A}(\sigma_{AB}) H_{\mu_A\sigma_B} c_{\sigma_A} c_{\sigma_B}}{t^{l_A}_{\mu_A}(\mu_A\nu_B) c_{\mu_A} c_{\nu_B}}} \quad (10)$$

Here, $c_{\sigma_A}\, c_{\sigma_B}$ is the coefficient of a model function different from $\mu_A\ \nu_B$, assuming the multiplicative separability of the zeroth order CASSCF function. Since H_0 and W are class-diagonal, the T_{AB}s appearing in the numerator can only be of the type 1. Let us start the iteration by taking the Ts in the zeroth iteration on the right of eq 10 to be just the converged amplitudes of the corresponding excitations from a group of core/active orbitals of A to active/virtual orbitals of A for the fragment function μ_A. We thus start $t^{l_A\,(0)}_{\mu_A}(\mu_A\ \nu_B) = t^{l_A}_{\mu_A}(\mu_A)$, for all μ_A and l_A and all ν_B. Then the numerator in eq 10 would look like $H^{l_A}_{\mu_A} + \{\overbrace{H^A_0 T_A(\mu_A)}\}^{l_A}_{\mu_A} - \{\overbrace{T_A(\mu_A) W_A}\}^{l_A}_{\mu_A}$. Since for type 1, with excitation on A, we have used converged amplitudes for the excitations on the fragment A, we have denoted these Ts as $T_A(\mu_A)$. For the denominator, we proceed in a similar manner. For a typical amplitude $t^{l_A}_{\mu_A}(\mu_A\nu_B)$ in eq 10, the denominator can be expanded as

$$\text{Denom} = E_{CAS_A} - H^0_{l_A l_A} + H^0_{\mu_A\mu_A} - H_{\mu_A\mu_A} + E_{CAS_B} - H_{\nu_B\nu_B} - (X_A + X_B) \quad (11)$$

with

$$X_A = \frac{-\sum_{\kappa_A\neq\mu_A} t^{l_A}_{\mu_A}(\kappa_A) H_{\mu_A\kappa_A} c_{\kappa_A} c_{\nu_B}}{t^{l_A}_{\mu_A}(\mu_A) c_{\mu_A} c_{\nu_B}} \quad (12)$$

and

$$X_B = \frac{-\sum_{\kappa_B\neq\nu_B} t^{l_A}_{\mu_A}(\mu_A) H_{\nu_B\kappa_B} c_{\mu_A} c_{\kappa_B}}{t^{l_A}_{\mu_A}(\mu_A) c_{\mu_A} c_{\nu_B}} \quad (13)$$

where again the zeroth iterates for $T_A(\mu_A)$ are used for the T_As. Since $c_{\nu B}$ cancels in the ratio of eq 12, X_A depends only on A. For X_B, we can use the eigenvalue equation for the fragment B

DOI: 10.1021/acs.jctc.5b00457
J. Chem. Theory Comput. 2015, 11, 4129−4145

for the coefficients on B in the active space on B as

$$X_B = \frac{-\sum_{\kappa_B} t^{l_A}_{\mu_A}(\mu_A) H_{\nu_B\kappa_B} c_{\mu_A} c_{\kappa_B} + t^{l_A}_{\mu_A}(\mu_A) H_{\nu_B\nu_B} c_{\mu_A} c_{\nu_B}}{t^{l_A}_{\mu_A}(\mu_A) c_{\mu_A} c_{\nu_B}}$$
$$= -E_{CAS_B} + H_{\nu_B\nu_B} \quad (14)$$

X_B cancels all the terms involving B in the denominator in eq 11, leading to

$$\text{Denom} = E_{CAS_A} - H^0_{l_A l_A} + H^0_{\mu_A\mu_A} - H_{\mu_A\mu_A} \quad (15)$$

The first iterate for $t^{l_A}_{\mu_A}(\mu_A\ \nu_B)$, $t^{l_A\,(1)}_{\mu_A}(\mu_A\ \nu_B)$ then takes the form

$$t^{l_A\,(1)}_{\mu_A}(\mu_A\nu_B) = \frac{H^{l_A}_{\mu_A} + \{\overline{H_0 T_{AB}}\}^{l_A}_{\mu_A} - \{\overline{T_{AB} W}\}^{l_A}_{\mu_A}}{E_{CAS_A} - H^0_{l_A l_A} + H^0_{\mu_A\mu_A} - H_{\mu_A\mu_A}} \quad (16)$$

The right side is just the expression for the converged amplitude $t^{l_A}_{\mu_A}(\mu_A)$. Thus, all the Ts of the type 1, with excitation on fragment A, will have the value of the converged cluster amplitudes the fragment function $\phi_{\mu A}$, and the situation remains unchanged on further iteration. Hence, we conclude that

$$t^{l_A\,(1)}_{\mu_A}(\mu_A\nu_B) = t^{l_A\,(1)}_{\mu_A}(\mu_A) \quad (17)$$

clearly indicating that, at the vanishing interfragment interaction limit, the cluster amplitudes involving excitations on A will not see the occupancy on the fragment B at all. The same conclusion also holds for excitations on B only. With the above analysis, it is straightforward to establish the relation

$$\tilde{H}^{\kappa_A\lambda_B}_{\mu_A\nu_B} = \tilde{H}_A{}^{\kappa_A}_{\mu_A}\delta_{\lambda_B\nu_B} + \tilde{H}_B{}^{\lambda_B}_{\nu_B}\delta_{\kappa_A\mu_A} \quad (18)$$

which displays the separability of the effective operator $\tilde{H}$ into two fragment energies involving A and B. Size-consistency of our UGA-SSMRPT2 is thus proven.

We would like to mention here that carefully chosen physically motivated size-consistency corrections such as in the perturbative formalism of Heully et al.[101] can be traced to approximations of rigorously formulated size-consistent theories. For example, the uncoupled SSMRCC (UC-SSMRCC) theory of Das et al.[102] who suggested an anonymous parentage approximation to the SSMRCC, where there are no coupling terms motivated by the desire of incurring low computational cost without losing size-consistency if used to generate its perturbative analogue, will automatically lead to a perturbative theory akin to the one by Heully et al.[101] in a class diagonal setting without the need for explicitly deleting the offending terms "by hand", so to say. Thus, Heully's formalism can be looked upon as the SSMRPT formalism in an "anonymous parentage" approximation with their zeroth order energy, E_0 taken as E_{CAS}.[63,65]

While exploring these aspects of size-consistency of various MRPTs, we were surprised to note that the asymptotes of some molecular PES, as obtained by MRMP2, show size-consistency, although MRMP2 can be shown to be size-inconsistent in general. We will analyze in the next subsection the reasons behind such unanticipated behavior.

An Aside: "Accidental" Size-Consistency of MRMP2 in Certain Situations. In this subsection, we look into what terms are responsible for the size-consistency error (SCE) in MRMP2 and in what condition we can have a zero error for the MRMP2 method. It can be analytically proved that the MRMP2 method is size-inconsistent. Rintelman et al.[103] first showed the size-inconsistency of the MRMP2 method numerically for noninteracting closed shell supermolecular systems, which has also been corroborated by Mao et al.[68] The size-inconsistency issue has not been sufficiently explored for molecular dissociation into open shell fragments, and we find that MRMP2 quite surprisingly, in several situations, displays exact size-consistency.

The H_0 for MRMP2 is the one particle generalized Fock operator. Conventional MRMP2 works with an H_0 which is strictly diagonal. This is a natural choice when working with canonical orbitals but is problematic for natural orbitals wherein the off-diagonal part of the generalized Fock operator would have to be considered as part of the perturbation. In our analysis, we consider the most general H_0 given by

$$H_0 = \sum_{p,q} f^q_p \hat{E}^q_p \quad (19)$$

where

$$f^q_p = h^q_p + \sum_{rs}\left(V^{qs}_{pr} - \frac{1}{2}V^{sq}_{pr}\right)D^s_r$$

and p, q, r, and s are orbitals in general; i and j are inactive occupied orbitals; u and v are active orbitals, and D^s_r represents the density matrix of the CAS function. The analysis for a strictly diagonal H_0 is easily subsumed in this framework. The zeroth order energy, E_0, for the MRMP2 method is given by

$$E_0 = \langle\Psi_0|H_0|\Psi_0\rangle \quad (20)$$

The second order energy correction is given by

$$E^{(2)} = \sum_l \frac{\langle\Psi_0|H|\chi_l\rangle\langle\chi_l|H|\Psi_0\rangle}{E_0 - H^0_{ll}} \quad (21)$$

χ_ls span the excited function space, which is generated by singles, doubles, etc. excitations from the configuration state functions (CSF)s spanning the reference function.

At infinite separation of a system, AB, into two fragments, A and B, the CASSCF function, Ψ_0, is product separable and can be written as

$$|\Psi_0\rangle = |\Psi_{0A}\Psi_{0B}\rangle \quad (22)$$

while the CASSCF energy is additive:

$$E_{CAS} = \langle\Psi_0|H|\Psi_0\rangle$$
$$= \langle\Psi_{0A}\Psi_{0B}|(H_A + H_B)|\Psi_{0A}\Psi_{0B}\rangle$$
$$= \langle\Psi_{0A}|H_A|\Psi_{0A}\rangle + \langle\Psi_{0B}|H_B|\Psi_{0B}\rangle$$
$$= E_{0A} + E_{0B} \quad (23)$$

Here, at fragment limit, the overlap between Ψ_{0A} and Ψ_{0B} is zero.

Now, let us consider the energy correction in eq 21 for a particular excitation case where only fragment A has been excited keeping fragment B intact:

Fragment A: $\mu_A \rightarrow l_A$

Fragment B: $\nu_B \rightarrow \nu_B$

The energy correction thus reduces to

$$E^{(2)} = \sum_{l_A} \frac{\langle\Psi_{0A}|H|\chi_{l_A}\rangle\langle\chi_{l_A}|H|\Psi_{0A}\rangle}{E_{0A} + E_{0B} - H^0_{l_A l_A} - H^0_{\nu_B\nu_B}} \quad (24)$$

DOI: 10.1021/acs.jctc.5b00457
J. Chem. Theory Comput. 2015, 11, 4129−4145

For the excitation of fragment A, where fragment B has remained unexcited, the MRMP2 correlation energy should solely depend on A. But it is evident from eq 24 that it has a contribution from fragment B and thus MRMP2 is size-inconsistent.

Now, we will try to investigate under what conditions MRMP2 can turn out to be size-consistent. For this, we concentrate only on the denominator, which is the source of the size-inconsistency, and recast is as

$$\Delta = (E_0 - H^0_{\mu\mu}) + (H^0_{\mu\mu} - H^0_{ll}) \tag{25}$$

where $(H^0_{\mu\mu} - H^0_{ll})$ is the orbital energy difference between the ground state and the excited function. $(E_0 - H^0_{\mu\mu}) = S_\mu$ is the energy difference between the zeroth order energy of the full function and that of the component CSFs, and this gives rise to the nonzero SCE. If S_μ for each reference function is zero, we will find that there will be no SCE for MRMP2.

$$\begin{aligned} S_\lambda &= E_0 - H^0_{\lambda\lambda} \\ &= \langle \Psi_0 | H_0 | \Psi_0 \rangle - \langle \phi_\lambda | H_0 | \phi_\lambda \rangle \\ &= \sum_{\mu\nu} c_\mu c_\nu \langle \phi_\mu | H_0 | \phi_\nu \rangle - \langle \phi_\lambda | H_0 | \phi_\lambda \rangle \\ &= \sum_{\mu\nu,\mathrm{pq}} c_\mu c_\nu f^q_p \langle \phi_\mu | E^q_p | \phi_\nu \rangle - \sum_{pq} f^q_p \langle \phi_\lambda | E^q_p | \phi_\lambda \rangle \\ &= \sum_{\mu\nu,\mathrm{pq}} c_\mu c_\nu f^q_p \gamma_{\mu\nu\ p}^{\ \ q} - \sum_{pq} f^q_p \gamma_{\lambda\lambda\ p}^{\ \ q} \\ &= \sum_{pq} f^q_p (D^q_p - \gamma_{\lambda\lambda\ p}^{\ \ q}) \\ &= \sum_{p} f^p_p (D^p_p - \gamma_{\lambda\lambda\ p}^{\ \ p}) + \sum_{p\neq q} f^q_p (D^q_p - \gamma_{\lambda\lambda\ p}^{\ \ q}) \end{aligned} \tag{26}$$

where,

$$D^q_p = \sum_{\mu\nu} c_\mu c_\nu \gamma_{\mu\nu\ p}^{\ \ q} \tag{27}$$

The orbital indices, p, in this equation can be classified into two classes:orbitals, p_d, which belong to groups, d, of energy levels, ϵ_d, and orbitals belonging to nondegenerate energy levels. The former class contributes to $S^{(I)}_\lambda$ and the latter contributes to $S^{(II)}_\lambda$. $S^{(III)}_\lambda$ corresponds to the off-diagonal term ($p \neq q$ term). In a given fragmentation limit with a given type of orbitals (natural, pseudocanonical, localized, etc.), MRMP2 will be size consistent only if the active orbitals, and their occupancy are such that $S^{(I)}_\lambda$, $S^{(II)}_\lambda$,and $S^{(III)}_\lambda$ are all zero for all λ. Thus, for size-consistency,

$$S_\lambda = S^{(I)}_\lambda + S^{(II)}_\lambda + S^{(III)}_\lambda = 0 \tag{28}$$

Possibility I: The degeneracy of the orbitals may occur due to symmetry (e.g., π_x and π_y orbitals for a linear molecule) or due to separability (e.g., π_x and π^*_x). For homonuclear molecules, both the Fock operator (f^q_p) and the density matrix (D^q_p) will be simultaneously diagonal at the asymptote, and D^q_p will be additionally a multiple of the unit matrix such that $\Sigma_{p_d} D^{p_d}_{p_d} = \Sigma_{p_d} n_{p_d} = N^d_e$, where n_{p_d} is the occupancy of the $p_d{}^{\mathrm{th}}$ orbital of energy ϵ_d, and N^d_e is the total number of electrons in this group of orbitals. Then $S^{(I)}_\lambda$ can be written as

$$\begin{aligned} S^{(I)}_\lambda &= \sum_d \epsilon_d \sum_{p_d} (D^{p_d}_{p_d} - \gamma_{\lambda\lambda\ p_d}^{\ \ p_d}) \\ &= \sum_d \epsilon_d (N^d_e - N^d_e) \\ &= 0 \end{aligned} \tag{29}$$

Possibility II: For nondegenerate orbitals, p,

$$S^{(II)}_\lambda = \sum_p f^p_p (D^p_p - \gamma_{\lambda\lambda\ p}^{\ \ p}) \tag{30}$$

If in the fragment limit, both the fragments have the same set of active orbitals with the same occupancy, then,

$$\begin{aligned} \gamma_{\mu\nu\ p}^{\ \ p} &= \langle \phi_\mu | E^p_p | \phi_\nu \rangle \\ &= \gamma_{\mu\mu\ p}^{\ \ p} \delta_{\mu,\nu}. \end{aligned} \tag{31}$$

Since the excitations involve the same orbitals, they can only differ in their spin-coupling scheme. Moreover, we know that $E^p_p |\phi_\nu\rangle = n^\nu_p |\phi_\nu\rangle$, and hence, $\langle \phi_\mu | E^p_p | \phi_\nu \rangle = n^\nu_p \delta_{\mu\nu}$, indicating that this matrix element exists only for the same model function on either side. It then follows that,

$$\begin{aligned} S^{(II)}_\lambda &= \sum_p f^p_p (D^p_p - \gamma_{\lambda\lambda\ p}^{\ \ p}) \\ &= \sum_p f^p_p \Big(\sum_{\mu\nu} c_\mu c_\nu \gamma_{\mu\nu\ p}^{\ \ p} - \gamma_{\lambda\lambda\ p}^{\ \ p} \Big) \\ &= \sum_p f^p_p \Big(\sum_{\mu} c^2_\mu \gamma_{\mu\mu\ p}^{\ \ p} - \gamma_{\lambda\lambda\ p}^{\ \ p} \Big) \end{aligned} \tag{32}$$

Thus, $S^{(II)}_\lambda$ vanishes if $\Sigma_\mu c^2_\mu \gamma_{\mu\mu\ p}^{\ \ p} = \gamma_{\lambda\lambda\ p}^{\ \ p}$. A very common situation of this type is where all the active orbitals are singly occupied, resulting in $\gamma_{\mu\mu p}^{\ \ p} = 1\ \forall\ p$ and $S^{(II)}_\lambda = 0$.

Possibility III: For the $p \neq q$ part of S_λ,

$$S^{(III)}_\lambda = \sum_{p\neq q} f^q_p (D^q_p - \gamma_{\lambda\lambda\ p}^{\ \ q}) \tag{33}$$

When pseudocanonical orbitals are chosen, $f^q_p = 0$ for $p \neq q$, and thus $S^{(III)}_\lambda$ will be zero, while for natural orbitals, on the other hand, the $D^q_p = 0$ for $p \neq q$. The $\gamma_{\lambda\lambda}$ is always diagonal, and therefore, when natural or pseudocanonical orbitals are used, $S^{(III)}_\lambda = 0$ always, and possibilities I or II or both can lead to accidental size-consistency of MRMP2.

ISSUES RELATED TO SIZE-CONSISTENCY IN UGA-SSMRPT2 AND RELATED MRPTS

As we have repeatedly emphasized, the success of any size-consistent multireference many body theory crucially depends on the correct asymptotic behavior and maintenance of symmetry of the zeroth order wave function. Thus, for MRPTs, their size-consistency is predicated by not only the size-consistency of the zeroth order CAS function but also the correctness of the orbitals in terms of their degeneracy and symmetry in the fragment limit, which plays an important role in ensuring the correct behavior of the dynamical correlation energy as introduced by the perturbative amplitudes.

Unlike all the SSMRCCs and UGA-SSMRCCs, which are invariant with respect to transformations within core and virtual orbitals, the corresponding perturbative analogues are

DOI: 10.1021/acs.jctc.5b00457
J. Chem. Theory Comput. 2015, 11, 4129−4145

not necessarily invariant with respect to transformation of core and virtual orbitals. This is dependent on the invariance of the unperturbed Hamiltonian, H_0, under the corresponding transformations. While one may imagine that all the SSMRCC/SSMRPTs will also be size-consistent in a straightforward manner with the use of localized orbitals, this unfortunately is not the case. As already emphasized by us in the first section, there may be potential pitfalls related to broken symmetric asymptotes in the zeroth order CAS functions which require careful explications and handling. In particular, the restrictions imposed by the standard softwares, which utilize the highest possible Abelian subgroup to classify the orbitals quite often prevent maintenance of the expected degeneracy of the fragment molecular orbitals. While this is an artifact of the orbital generation procedure, this might lead to loss of size-consistency of an otherwise size-extensive theory in practical applications. To bypass or at least to ameliorate the loss of size-consistency in such situations, we need to look carefully at ways to restore the expected degeneracy. Another distinct but related issue is to ensure the compatibility of the fragment orbitals, computed separately with the fragments, with those of the supermolecule in the fragmentation limit. It might so happen that we have to abandon optimizing the orbitals via a CASSCF procedure for some molecular states to achieve this compatibility. We itemize and delineate below all these issues in detail, with illustrative examples whenever necessary. In an MRPT based on CAS, the orbitals are usually (though not always[104]) generated by a CASSCF procedure. In our case, since we make use of the unitary group to preserve spin-symmetry, we have chosen to use the GUGA-CASSCF module of GAMESS-US.[105] The most commonly encountered problem for GUGA-CASSCF is related to the necessity of using an Abelian point group for orbital optimizations. At the fragmentation limit, this may result in a loss of degeneracy of the orbitals, which should be degenerate by symmetry. For example, the p orbitals of an atom as a fragment should be triply degenerate, but for atoms with p^1, p^2, p^4, and p^5 electronic configurations, they cease to be so. We call the fragment/supermolecular states having such orbitals as symmetry broken.

While dealing with symmetry broken states in the fragment limit, even the issue of size-consistency of a CASSCF wave function is tricky. The CASSCF continues to be size-consistent only if the nature of symmetry breaking of the fragments coincides with that of the supermolecule. This hinges on the symmetry axes selected for the two computations as well as on the idiosyncrasies of the numerical procedures. This is a primary requirement for us to have a chance to demonstrate the size-consistency of any MRPT.

Remember that Ψ_0 is invariant to all class-wise orbital rotations, while the ϕ_μs are not; ϕ_μs have only restricted invariance under transformation of core and virtual orbitals separately. This would spell an invariance in SSMRPT with respect to these transformations only if the H_0 has a similar invariance. Since any class diagonal H_0 in SSMRPT maintains the restricted invariance of the ϕ_μs, our choice for H_0 as class-diagonal makes the UGA-SSMRPT2 invariant in this restricted sense. It is pertinent to mention here that a fully diagonal as opposed to class-diagonal H_0 as a possible choice in our UGA-SSMRPT2 (or as in SA-SSMRPT of Mao et al.[67]) would lead to a breakdown of this property. On the other hand, the use of an H_0 as proposed by Dyall[106] would lead to invariance for transformations among active orbitals as well. In fact, such a zeroth order Hamiltonian has been used with SSMRPT by Evangelista et al.[66] for (2,2) CAS, but since the ϕ_μs are still noninvariant, the theory overall is not orbital invariant. If the core and virtual orbitals of the fragments and the supermolecule are related by orthogonal transformations rather than being identical, a loss of size-consistency would be seen when using a diagonal H_0 in spite of the manifest size-extensivity of the theories. This phenomenon commonly occurs for homonuclear diatomics where the core and virtual orbitals remain delocalized for the supermolecule, while in the fragments computed separately they are by necessity localized. We have encountered such a situation for the $1^1\Pi_u$ state of C_2. Clearly, the choice of a fully diagonal H_0 is not an option for maintaining size-consistency.

On the other hand, our UGA-SSMRPT2 cannot be invariant with respect to rotations of active orbitals. The use of localized orbitals is advocated for ensuring size-consistency in these cases. Localization techniques have their own limitations. First, to ensure the localizability of the active orbitals, a suitable point group lower than that necessary for generation of delocalized orbitals must be chosen. A practical difficulty faced by us is the necessity for carrying out the orbital optimization and localization of the active orbitals in a single CASSCF run for example in GAMESS-US used by us. This sometimes leads to the generation of core and virtual orbitals, which are rotated with respect to the delocalized orbitals originally obtained. This situation may give rise to the pathology of "rotated core" and "rotated virtuals" differentiating the behavior of the MRPTs with diagonal and class-diagonal H_0s mentioned in the previous paragraph. We have encountered such a situation for the $1^3\Sigma_g^-$ state of O_2.

A further possible hurdle to the size-consistency of a noninvariant MRPT is the effect of the difference in the nature of symmetry breaking of the active orbitals in the fragments and the supermolecule. If the difference is only a rotation within the active orbitals then the size-consistency of CASSCF is not affected. However, due to the interdependence of the active and inactive orbitals during the orbital optimization procedure, this also reflects on the core and virtual orbitals. Due to the noninvariance of the ϕ_μs and the cluster amplitudes, the MRPT would then turn out to be size-inconsistent. This problem can be overcome by a further rotation of the active orbitals of the supermolecules such that they resemble those of the fragments at the asymptote, but how this would translate from the noninteracting to the interacting region of the PES cannot be discerned *a priori*.

A possible way for the restoration of expected degeneracies where the CASSCF function turns out to be broken symmetric is to optimize a CAS function, which is an equally weighted combination of the set of symmetry broken states which ought to have been degenerate at the asymptote. If these lie in the same irreducible representation (IRREP) of the Abelian subgroup being used, this can be carried out easily by what is called a state averaged GUGA-CASSCF (SA-CASSCF). For ease of reference in our future discussions, we refer to this as **Procedure I** for symmetry restoration. On the other hand, if the states to be averaged lie in different IRREPs of the Abelian subgroup, this is not possible in the GUGA module of current software packages. State-averaging carries the price that the orbitals are no longer fully optimized for the state of interest and may be poor for tracing the full PES of these states owing to their energetic separation at various parts of the PES. This procedure can be adopted without difficulty when the states we are averaging lie reasonably close to each other throughout the PES. We have adopted this not only in such situations but also in others paying

DOI: 10.1021/acs.jctc.5b00457
J. Chem. Theory Comput. 2015, 11, 4129−4145

the price of a poorly described interaction region since our focus was principally on the size-consistency.

An alternative procedure for a more balanced description of a PES may be to use orbitals of a close lying state, albeit of a different space-spin symmetry, which gives the same asymptotic limit for the full PES. The orbitals, in this case, may also be obtained from an SA-CASSCF of that space-spin symmetry. We call this **Procedure II**. We have used Procedure II for certain applications, viz., for the $1^3\Sigma_g^-$ state of O_2 and the $1^1\Pi_u$ state of C_2. UGA-SSMRPT2 (and other size-extensive SSMR theories) with such symmetry-restored zeroth order CASSCF functions easily preserve size-consistency with the additional requirement of localized orbitals when the theory is not orbital invariant. We feel that studies on size-consistency will greatly benefit if softwares generating localized CASSCF orbitals are made available as open source codes. The works of the group of Malrieu[107,108] have indeed produced such codes, although they are not popular as yet.

NUMERICAL INVESTIGATION OF SIZE-CONSISTENCY OF MULTIPLY BONDED MOLECULES

In this section, we have carried out a thorough investigation of the numerical demonstration of size-consistency of our recently developed UGA-SSMRPT2 method using prototypical small linear molecules with pronounced multireference character. We have studied the lowest state of various space-spin symmetries for a set of 14 electron molecules namely, N_2, C_2H_2, and HCN. For O_2 and C_2, the ground and some closely lying excited states with interesting features in their PES have been chosen. An extensive study of the PES and spectroscopic parameters with the spinorbital-based SSMRPT[63] using a diagonal H_0 has been carried out for some of the molecules[109−111] we have chosen and is found to be very promising.

We do not pursue a similar comparative study as we only wish to elucidate our general findings enlisted in the previous section. For a benchmark study of UGA-SSMRPT2 vis-á-vis FCI and other PTs, we would like to refer the readers to our earlier publication.[69] Our findings indicate that PES computed using UGA-SSMRPT2 show more parallelity with those obtained from FCI and are also less erratic in behavior across the PES when compared with MRMP2 or the MCQDPT2 numbers. In addition, we may mention that since localized orbitals perform somewhat poorly at the equilibrium but very well at the asymptote, the quality of PES in terms of NPE and MAD is poorer in case of localized orbitals vis a vis natural orbitals.

All the UGA-SSMRPT2 computations have been done with localized orbitals where the Pipek−Mezey localization scheme[112] has been adopted. On the other hand, for the MRMP2 computations, delocalized pseudocanonical orbitals are used since it was not developed for localized orbitals as implemented in GAMESS-US.[105] All the CASSCF, CASCI, and MRMP2 computations have been done using the GAMESS program package.[105]

The molecular applications can be considered to be in two categories. In the first, we have studied the fragment limit of some molecules where the fragments have orbitals which are degenerate for symmetry reasons. For example, in situations where both the fragments have $2p^3$ configurations, equivalence between $p_i(i = x,y,z)$ orbitals automatically follows. The ground state of nitrogen and some of the excited states of C_2H_2 and HCN belong to this category where all the active orbitals are degenerate and singly occupied. In the second category, there are molecular states with fragments which should have had certain degeneracies by virtue of their symmetries, but this fails to be realized due to one or more of the reasons explained in the previous section. The aspect of size-consistency, as revealed by our computation, is therefore to be accepted with some qualifications. The MRMP2 results turn out to be size-consistent for all states in the first category and some specific situations in the second category. This behavior has been amply explained in the previous section, and our results numerically verify our conclusions in this regard. Pseudocanonical orbitals have been used for all MRMP2 computations and thus $S_\lambda^{(III)} = 0$ in all cases. Our UGA-SSMRPT2 is found to be manifestly size-consistent in all fragmentations of both first and second category, viz., irrespective of whether the asymptotic supermolecule wave function has proper symmetry or broken symmetry. The numerical threshold for the convergence is set to be $10^{-2}\mu E_h$ in all our computations, and the size-consistency of UGA-SSMRPT2 is found to be satisfied up to this threshold.

Molecule: N_2. The ground state PES of N_2 requires a a minimal CAS(6,6) with a corresponding CAS(3,3) for the N atom to describe it properly. The ground state of the nitrogen atom is a ^4S, where the three electrons occupy three degenerate p orbitals. A close-lying ^2D state of the nitrogen atom consists of one doubly occupied orbital, one singly occupied orbital, and an unoccupied orbital. The optimized CASSCF for the ^4S state is perfectly symmetric but that for ^2D is not. We could have used Procedure I for restoring the symmetry of the ^2D state, but this is not necessary for our purposes as we are interested only in investigating the size-consistency of the lowest states in each space-spin symmetry going over to the three lowest fragmentation limits of N_2.

These states are categorized in terms of their atomic fragments as the following:

$$\begin{aligned} 1^1\Sigma_g^+,\ 1^3\Sigma_u^+,\ 1^5\Sigma_g^+ &\rightarrow {}^4S + {}^4S \\ 1^3\Delta_u,\ 1^3\Pi_g,\ 1^5\Pi_u &\rightarrow {}^4S + {}^2D \\ 1^1\Sigma_u^- &\rightarrow {}^2D + {}^2D \end{aligned} \tag{34}$$

Although the N_2 molecule belongs to the $D_{\infty h}$ point group, the D_{2h} point group is adopted for obtaining the delocalized orbitals and the C_{2v} point group is adopted for localization. The ground state, $1^1\Sigma_g^+$, dissociates into two ^4S states with three equivalent molecular orbitals on each fragment. $1^3\Sigma_u^+$ and $1^5\Sigma_g^+$ states, which also separate into the same fragments, have similar properties as stated above. Thus, the CASSCF orbitals for these three states are perfectly symmetry adapted, and size-consistency is easily demonstrated both at the zeroth order (CASSCF) and for UGA-SSMRPT2.

For $1^3\Delta_u$, $1^3\Pi_g$, and $1^5\Pi_u$ at the fragment limit, three symmetry broken molecular orbitals, with occupancies of 2, 1, and 0, respectively, are centered on the fragment 1 indicating the correspondence of fragment 1 with the symmetry broken ^2D state of the N atom, while the rest of the molecular orbitals are equivalent among themselves with occupancies of 1, 1, and 1, respectively, and are centered on the fragment 2, indicating that they comprise the ^4S state of the other N atom. Similarly, the $1^1\Sigma_u^-$ state is comprised of two symmetry broken N atoms in their ^2D states at the fragment limit.

For all the asymptotes, UGA-SSMRPT is found to be size-consistent below the convergence threshold ($10^{-2}\mu E_h$). The MRMP2 method is found to give size-consistent results in all the states above. The reason for this surprising behavior has been explained in the previous section: the situation falls in Possibility I for the $^4S + {}^4S$ asymptote and is a combination of Possibilities I

DOI: 10.1021/acs.jctc.5b00457
J. Chem. Theory Comput. 2015, 11, 4129−4145

Table 1. N_2 Molecule: Size-Consistency Check with cc-pVDZ Basis Set[a]

	N atom		N_2 molecule		
	^4S	^2D	$^4S + {}^4S$	$^2D + {}^2D$	$^4S + {}^2D$
	^4S	^2D	$1^1\Sigma_g^+$, $1^3\Sigma_u^+$, $1^5\Sigma_g^+$	$^1\Sigma_u$	$1^3\Delta_u$, $1^3\Pi_g$, $1^5\Pi_u$
CASSCF	−54.3884142	−54.2826977	−108.7768285	−108.5653955	−108.671112
SCE			[b]	[b]	[b]
UGA-SSMRPT2	−54.4618289	−54.3618231	−108.9236578	−108.7236462	−108.8236520
SCE			[b]	[b]	[b]
MRMP2	−54.4735446	−54.3738504	−108.9470892	−108.7477008	−108.8473950
SCE			[b]	[b]	[b]

[a]Localized orbitals are used for UGA-SSMRPT2 computations. [b]Below convergence threshold ($10^{-2}\mu E_h$).

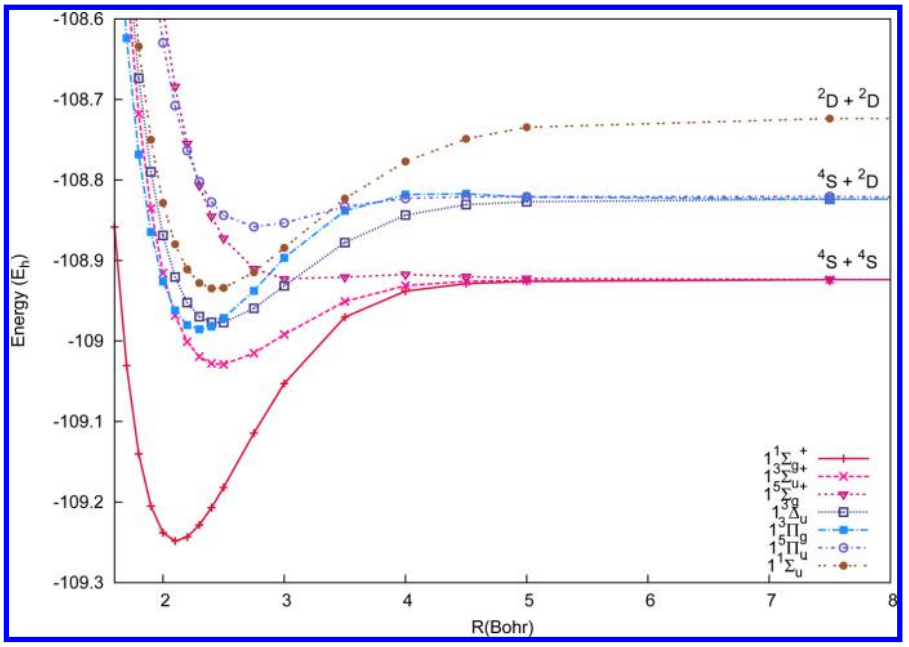

Figure 1. PES of N_2 computed with cc-pVDZ basis using UGA-SSMRPT2.

and II for the two other asymptotes. The size-consistency errors for different methods have been tabulated in Table 1.

The PES of these seven states are shown in Figure 1. For the nitrogen molecule, we see that the ground state remains the lowest energy state all the way up to dissociation. All the excited states of the nitrogen molecule studied by us are quite strongly bound states around their respective equilibrium geometry indicating its strong bonding.

Molecule: C_2H_2. Acetylene (C_2H_2) is isoelectronic with the nitrogen molecule, and the CH radical is isoelectronic with the N atom. Similar to the N atom ($[(1s^2 2s^2)_{core} 2p^3]$), the CH radical also has seven electrons which give rise to CH($^4\Sigma$), CH($^2\Pi$), and CH($^2\Delta$). Acetylene is also a triple-bonded system, where a CAS(6,6) is sufficient to show the proper dissociation of the various states of the molecule. But unlike the N atom, here we obtain a different energy ordering of the atomic fragments as CH($^2\Pi$) < CH($^4\Sigma^+$) < CH($^2\Delta$). As a result, the energy ordering of the molecular asymptotes is also different from those of N_2. In our studies, we have considered some of the molecular states of C_2H_2 going over to the $^2\Pi$ and $^4\Sigma^+$ fragments as listed below:

$$
\begin{aligned}
1^1\Sigma_u^-,\ 1^3\Sigma_u^- &\rightarrow {}^2\Pi + {}^2\Pi \\
1^3\Pi_g,\ 1^5\Pi_u &\rightarrow {}^4\Sigma^+ + {}^2\Pi \\
1^1\Sigma_g^+,\ 1^3\Sigma_u^+,\ 1^5\Sigma_g^+ &\rightarrow {}^4\Sigma^+ + {}^4\Sigma^+
\end{aligned}
\qquad (35)
$$

The CH bond distance has been kept fixed at 1.0697984 Å, and localized orbitals in a C_{2v} point group are used. The $^4\Sigma^+$ state of the CH radical is very similar to the nitrogen atom where there are three singly occupied active orbitals. Here, we have considered the $1^1\Sigma_g^+$, $1^3\Sigma_u^+$, and $1^5\Sigma_g^+$ states, which are all bound and go to the same asymptotic limit ($^4\Sigma^+ + {}^4\Sigma^+$), although the depths of the potential wells get shallower and the binding energies become less for the states of higher spin-multiplicity. Though the $1^1\Sigma_g^+$ state is the ground state at the equilibrium region, it no longer remains the lowest energy state at the fragment limit. The $1^1\Sigma_u^-$ and $1^3\Sigma_u^-$ states, which go over to two $^2\Pi$ states of CH at the asymptote, become the lowest energy states at the fragment limit. Starting from dissociation, these states slowly rise up and then suddenly go down to minima indicating avoided curve crossings in that region. We have found that the $1^3\Pi_g$ and $1^5\Pi_u$ states go to another asymptotic level $^4\Sigma^+ + {}^2\Pi$, which lies between the above two fragment limits. These states are also found to be bound. All the PES are shown in Figure 2 clearly indicating the asymptotic region in an inset. The crossing of the states belonging to the $^4\Sigma^+ + {}^4\Sigma^+$ limit and the $^2\Pi + {}^2\Pi$ limit is shown in another inset where the latter states come down under the former states.

As explained in the theory section, the accidental size-consistency of MRMP2 of various states largely depend on the occupancy of the states at the dissociation or in other words occupancy of the individual fragments. The states going to the

DOI: 10.1021/acs.jctc.5b00457
J. Chem. Theory Comput. 2015, 11, 4129−4145

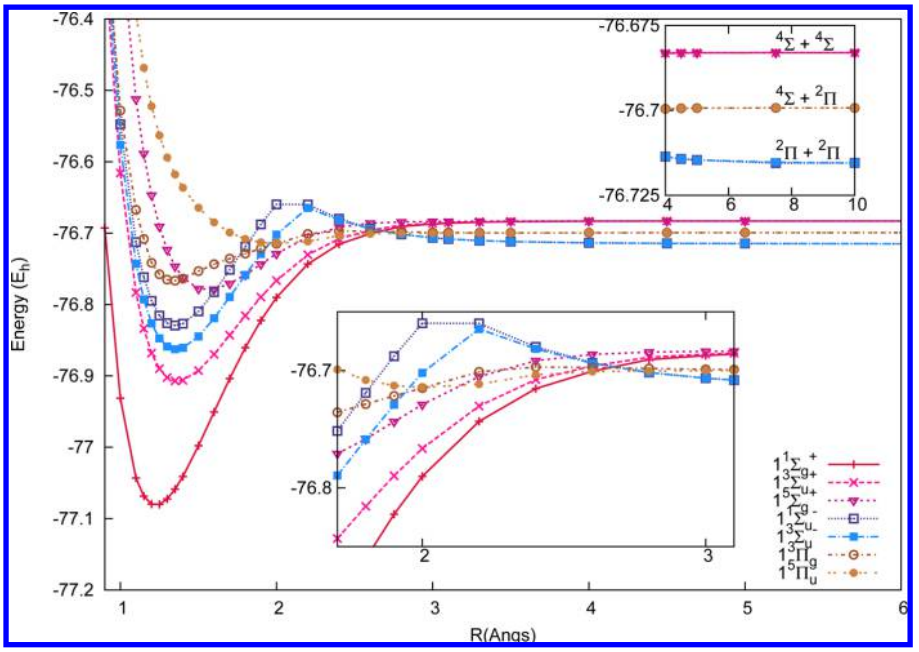

Figure 2. PES of C_2H_2 computed with cc-pVDZ basis using UGA-SSMRPT2. The upper inset shows a close-up of the asymptotic region and the lower inset shows the region of multiple curve crossings.

Table 2. C_2H_2 Molecule: Size-Consistency Check with cc-pVDZ Basis Set[a]

	CH molecule			C_2H_2 molecule		
	$^2\Pi$	$^4\Sigma$	$^2\Delta$	$1^1\Sigma_u^-$, $3^1\Sigma_u^-$	$1^3\Pi_g$, $1^5\Pi_u$	$1^1\Sigma_g^+$, $1^3\Sigma_u^+$, $1^5\Sigma_g^+$
	$^2\Pi$	$^4\Sigma$	$^2\Delta$	$^2\Pi + {}^2\Pi$	$^2\Pi + {}^4\Sigma$	$^4\Sigma + {}^4\Sigma$
CASSCF	−38.2888609	−38.2793846	−38.1681557	−76.5777216	−76.5682455	−76.5587693
SCE				[b]	[b]	[b]
UGA-SSMRPT2	−38.3577879	−38.3415158	−38.2441513	−76.7155757	−76.6993036	−76.6830315
SCE				[b]	[b]	[b]
MRMP2	−38.3636594	−38.3507867	−38.2590169	−76.7283399	−76.7149891	−76.7015734
SCE				1.021 mE_h	0.543 mE_h	[b]

[a]Localized orbitals are used for UGA-SSMRPT2 computations. [b]Below convergence threshold ($10^{-2}\mu E_h$).

$^4\Sigma^+ + {}^4\Sigma^+$ limit each have six singly occupied active orbitals and as expected from of our analysis MRMP2 shows size-consistency by virtue of Possibility II. Occurrence of $^2\Pi$ in the fragment limit destroys this fortuitous behavior of MRMP2 for the rest of the states studied. In the latter set of states, the size-consistency error of MRMP2 is found to be around $0.5mE_h$, whereas UGA-SSMRPT is size-consistent below the convergence threshold ($10^{-2}\mu E_h$) always (Table 2).

Molecule: HCN. The HCN molecule is also isoelectronic with the N_2 and C_2H_2 molecule. Likewise, HCN is also a triple bonded system which can be best described by taking a CAS(6,6). We have studied the fragmentation limit of HCN to CH and N, where CH bond distance is kept fixed at 1.0697984 Å throughout the PES. As we have seen earlier, the ^4S state of the nitrogen atom is the ground state and is perfectly symmetric while the ^2D state is symmetry broken. On the contrary, $^2\Pi$ is the lowest but symmetry broken ground state for the CH radical whereas the next highest $^4\Sigma$ state is of proper symmetry. Here, we have studied some of the combination states of CH and N from each fragments as listed below:

$$
\begin{aligned}
1^3\Pi,\ 1^5\Pi &\rightarrow {}^4S(N) + {}^2\Pi(CH)\\
1^1\Sigma^+,\ 1^3\Sigma^+,\ 1^5\Sigma^+ &\rightarrow {}^4S(N) + {}^4\Sigma^+(CH)\\
1^1\Pi &\rightarrow {}^2D(N) + {}^2\Pi(CH)
\end{aligned}
\qquad (36)
$$

The molecular states composed of the broken symmetry fragments are also broken symmetric at the fragment limit. We have chosen to follow the broken symmetry asymptotes for our selection of states, which are the lowest in their space-spin symmetries. As the energy ordering of the nitrogen atom and CH radical suggests, $^4S(N) + {}^2\Pi(CH)$ is the lowest asymptotic fragment. $1^3\Pi$ and $1^5\Pi$ states go to this fragment limit. Starting from the dissociation, both these states are degenerate up to almost 2.0 Å, after which they split. The $1^3\Pi$ state is a bound state at the equilibrium region (1.25 Å) showing a big hump at around 1.7 Å, indicating an avoided curve crossing with a higher lying state of the same symmetry. The $1^5\Pi$ state seems to be an unbound state, which rises slowly as we go from dissociation to equilibrium and eventually gets affected by other low lying states. The $1^1\Sigma^+$,$1^3\Sigma^+$, and $1^5\Sigma^+$ states go to the $^4S(N) + {}^4\Sigma(CH)$ asymptote. All these three states are found to be bound states. We have studied another state $1^1\Pi$, which goes to a different fragment limit ($^2D(N) + {}^2\Pi(CH)$). The $1^1\Pi$ state is also an unbound state, and as it gets near the equilibrium, it gets affected by other low lying states. We have only computed the lowest energy state of singlet Π symmetry, $1^1\Pi$, as shown in Figure 3 and did not try to trace the various crossovers involving the higher lying $^1\Pi$ states in shaping the PES.

Results related to size-consistency of the different methods are presented in Table 3. The UGA-SSMRPT method is found

DOI: 10.1021/acs.jctc.5b00457
J. Chem. Theory Comput. 2015, 11, 4129−4145

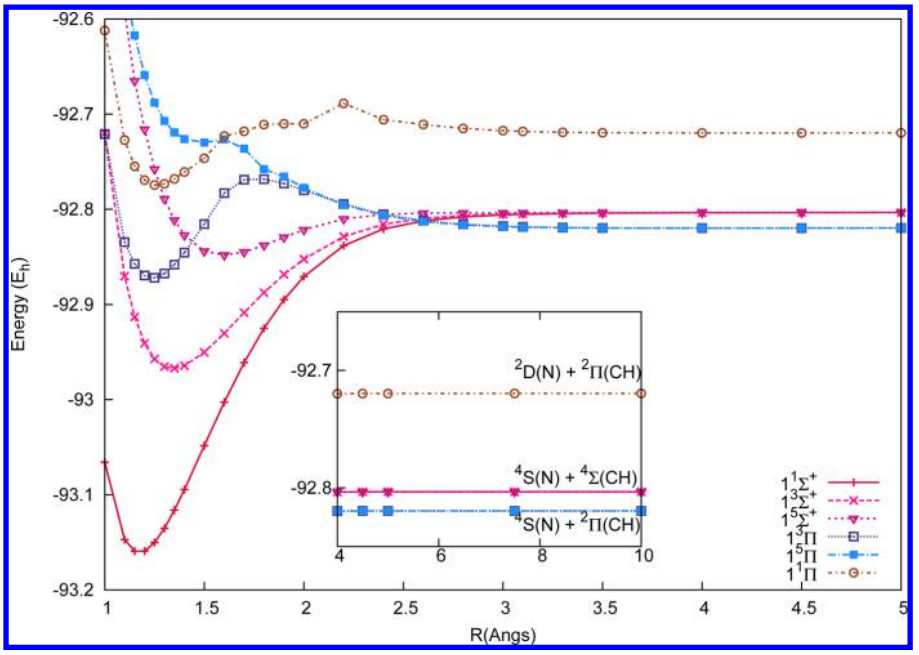

Figure 3. PES of HCN computed with cc-pVDZ basis using UGA-SSMRPT2. The asymptotic region is focused in the inset.

Table 3. HCN Molecule: Size-Consistency Check with cc-pVDZ Basis Set[a]

	N atom		CH molecule		HCN molecule		
	^4S	^2D	$^2\Pi$	$^4\Sigma$	$1^3\Pi$, $1^5\Pi$	$1^1\Sigma^+$, $1^3\Sigma^+$, $1^5\Sigma^+$	$1^1\Pi$
	^4S	^2D	$^2\Pi$	$^4\Sigma$	$^4S + ^2\Pi$	$^4S + ^4\Sigma$	$^2D + ^2\Pi$
CASSCF	−54.3884142	−54.2826977	−38.2888609	−38.2793846	−92.6772756	−92.6677985	−92.5715586
SCE					[b]	[b]	[b]
UGA-SSMRPT2	−54.4618289	−54.3618231	−38.3577879	−38.3415158	−92.8196167	−92.8033446	−92.7196115
SCE					[b]	[b]	[b]
MRMP2	−54.4735446	−54.3738504	−38.3636594	−38.3507867	−92.8376176	−92.8243313	−92.7470194
SCE					0.414 mE_h	[b]	0.444 × $10^{-5}mE_h$

[a]Localized orbitals are used for UGA-SSMRPT2 computations. [b]Below convergence threshold ($10^{-2}\mu E_h$).

to be size-consistent for all the asymptotes studied here. Size-consistency of the MRMP2 method follows from our analysis in the theory section. The $1^1\Sigma^+$, $1^3\Sigma^+$, $1^5\Sigma^+$ states, which are composed of ^4S of nitrogen and $^4\Sigma$ of the CH radical, are found to be size-consistent since both the fragments consist of three singly occupied orbitals each, resulting in six electrons in six orbitals for HCN. This leads to size-consistency for the MRMP2 method by virtue of Possibility II. On the contrary, $1^1\Pi$, $1^3\Pi$, and $1^5\Pi$ give nonzero size-consistency errors for MRMP2 since they do not correspond to any of the possibilities discussed in the previous section. The $1^1\Pi$ state involves ^2D of nitrogen (occupancy = 210) and $^2\Pi$ of CH (occupancy = 210), and the $1^3\Pi$ and $1^5\Pi$ states involve $^2\Pi$ of CH with occupancy 210 and ^4S of nitrogen with occupancy 111.

Molecule: O_2. O_2, though small, displays several pathologies in realizing size-consistency in a convincing manner, and thus, the theoretical considerations delineated in the previous sections have to be carefully considered. Its ground state is a triplet rather than a singlet, contrary to the most common occurrence for ground states of molecules with even number of electrons. More importantly, as we will discuss in some detail, the asymptote of the ground state PES of the oxygen molecule consists of broken symmetric active orbitals on each oxygen atom, in the CASSCF computation.

The electronic configuration of a ground state oxygen atom is $[(1s^2)_{core}2s^22p^4]$. Here, we have considered both the 2s and 2p orbitals as active orbitals constituting a CAS(12,8) with 12 electrons in 8 orbitals for the oxygen molecule and correspondingly a CAS(6,4) for the oxygen atom. If we perform the computation on an isolated atomic oxygen, in a D_{2h} or in a C_{2v} point group, the CASSCF orbitals are optimized corresponding to the configuration $2s^22p_z^22p_x\ 2p_y$. This is clearly a symmetry broken solution where the equivalence of the p_z orbital with p_x and p_y is lost, and the expected degeneracy of a ^3P is not realized. We can restore the symmetry of the O atom by Procedure I. Due to the limitation of the GAMESS package, this can be done only in the C_1 point group and taking a state-averaging of the three states arising from p_x, p_y, and p_z. They lead to p orbitals which are not pure p_x, p_y, or p_z, but they remain degenerate and therefore do not pose a problem since it is an isolated atom and not a molecule.

For the O_2 molecule, the three lowest states around their respective equilibrium regions are $1^3\Sigma_g^-$, $1^1\Delta_g$, and $1^1\Sigma_g^+$ according to their energy ordering, which are all degenerate in the fragment limit of $^3P + ^3P$. According to Procedure I, we have selected $1^1\Delta_g$, $1^1\Sigma_g^+$, and $2^1\Sigma_g^+$ states for obtaining the symmetry restored orbitals for this set of singlet states which belong to the same representation (A_1) in the Abelian subgroup of

DOI: 10.1021/acs.jctc.5b00457
J. Chem. Theory Comput. 2015, 11, 4129−4145

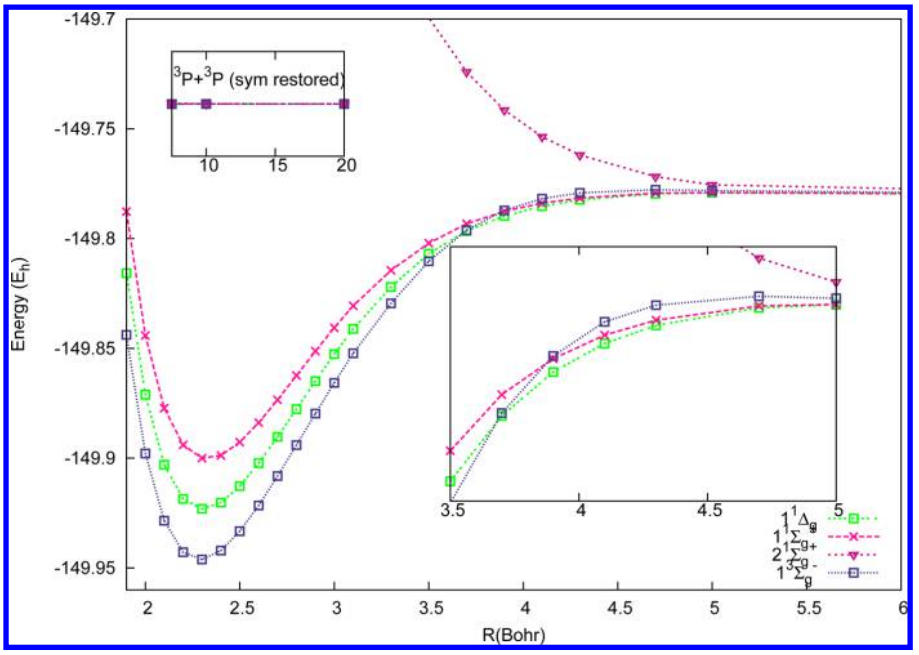

Figure 4. PES of O_2 computed with cc-pVDZ basis using UGA-SSMRPT2. The region of multiple curve crossing is focused in the inset.

$D_{\infty h}$, the C_{2v} point group which is used in this computation. The $2^1\Sigma_g^+$ state is, however, found to be an unbound state. The CASSCF energy of these states at the fragment limit is twice of the CASSCF energy of the symmetry restored oxygen atom.

On the other hand, the $1^3\Sigma_g^-$ state cannot be easily obtained by Procedure I as the states which ought to have been averaged are energetically widely dispersed. Still, as mentioned above, one can show the degeneracy of this state at the fragment limit with the other states by using the same state averaged orbitals as for the singlet states, i.e., Procedure II. Unfortunately, further orbital optimization for this state will lead again to a broken symmetric solution, and hence, only a CASCI with these state-averaged orbitals is carried out for the $1^3\Sigma_g^-$ state to generate the zeroth order function before we can initiate the correlation calculation. Thus, we see that we have to compromise with the fact that we cannot have a symmetry restored solution, while simultaneously generating optimized orbitals for each individual state.

Another issue, which is of concern while verifying size-consistency, is the treatment of symmetry broken orbitals in the fragment limit when the core/virtual orbitals are generated in a localized manner but are not the same as those on the isolated O atoms. It so happens that the core/virtual orbitals of the supermolecule at the fragmentation limit are related by orbital rotations among the core and virtual orbitals separately with the core/virtual orbitals on the isolated atom for the ground state of O_2. More interestingly, the active orbitals containing the 2s basis, generated by the Pipek−Mezey localization, also emerge as different from the 2s orbital on the isolated O. Since there is only one s orbital on the isolated O atom, the Pipek−Mezey localization constraint does not affect this orbital. But for the supermolecule, there are two orbitals with 2s, a bonding and an antibonding, and the Pipek−Mezey localization generates a pair of orbitals different from the atom. Hence, we also induce a rotation between the two 2s type orbitals for the supermolecule such that they look like the 2s orbital of the fragment. The expected size-consistency of our UGA-SSMRPT2 with the appropriately localized core/virtual and active orbitals is then restored. Such rotations have no effect on the zeroth order energy, but the corresponding UGA-SSMRPT2 results would violate size-consistency unless the extra rotations on the active orbitals are performed, although with a class-diagonal H_0, the rotated core and virtual orbitals pose no problem.

In Figure 4, we have plotted the PES of the symmetry restored $1^3\Sigma_g^-$, $1^1\Delta_g$, $1^1\Sigma_g^+$, and $2^1\Sigma_g^+$ states. As depicted in Figure 4, the $1^3\Sigma_g^-$ state is the ground state which crosses the $1^1\Delta_g$ and $1^1\Sigma_g^+$ states at around 3.5−4.0 au, eventually going to the same asymptote. Our UGA-SSMRPT2 theory is found to be size-consistent, while the SCE for MRMP2 method is around 0.497 mE_h, as shown in Table 4.

Molecule: C_2. Despite its small size, C_2 poses a real theoretical challenge. There are a large number of low-lying

Table 4. O_2 Molecule: Size-Consistency Check with cc-pVDZ Basis Set[a]

	O atom	O_2 molecule
	^3P	$1^3\Sigma_g^-$, $1^1\Delta_g$, $1^1\Sigma_g^+$
	^3P	$^3P + {}^3P$
symmetry broken wave function		
CASSCF	−74.7875131	−149.5750261
SCE		[b]
UGA-SSMRPT2	−74.8949593	−149.7899186
SCE		[b]
MRMP2	−74.9039179	−149.8076032
SCE		0.2368mE_h
symmetry restored wave function		
CASSCF	−74.7861880	−149.5723760
SCE		[b]
UGA-SSMRPT2	−74.8901210	−149.7802420
SCE		[b]
MRMP2	−74.9031653	−149.8068279
SCE		0.4973mE_h

[a]Localized orbitals are used for UGA-SSMRPT2 computations. [b]Below convergence threshold ($10^{-2}\mu E_h$).

DOI: 10.1021/acs.jctc.5b00457
J. Chem. Theory Comput. 2015, 11, 4129−4145

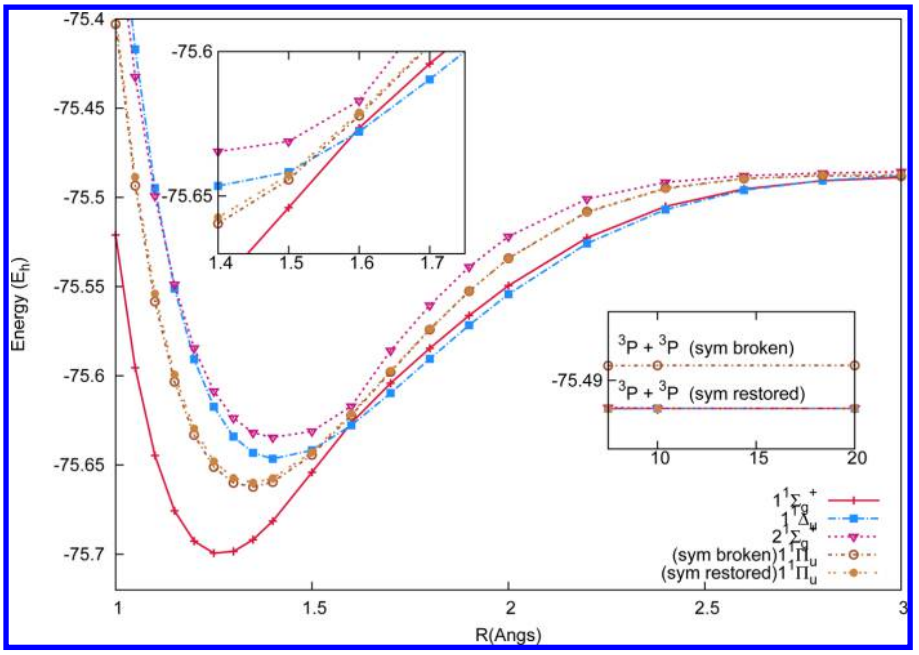

Figure 5. PES of C_2 computed with cc-pVDZ basis using UGA-SSMRPT2. The region of multiple curve crossing is focused in the inset.

excited states which lead to several avoided curve crossings. Moreover, even the ground state has strong multireference character. Since single reference theories completely fail to explain the bonding in C_2, this is a very good testing ground for the various multireference methods. There are lots of studies (and conceptual controversies)[113] related to the nature of bonding in C_2.

The ground state of C_2 is $^1\Sigma_g^+$ at equilibrium, which dissociates into two carbon atoms in the ^3P state. The electronic configuration of the ground state carbon atom is $[(1s^2)_{\text{core}}\ 2s^2 2p^2]$. In C_2, both 2s and 2p orbitals participate in bonding, making one σ and two Π bonds with two electrons remaining on the carbon atoms. A CAS(8,8) is an appropriate space for accommodating these active electrons in these orbitals. Correspondingly, a CAS(4,4) is chosen for the atom.

As in the O atom, Procedure I is adopted for the ^3P state of the C atom using a C_1 point group. Two electrons are distributed equivalently among three equivalent p_x, p_y, and p_z orbitals, giving a symmetry restored solution for C.

Interestingly, there are four singlet states of C_2, $1^1\Sigma_g^+$, $1^1\Delta_g$, $2^1\Sigma_g^+$, and $1^1\Pi_u$, which go over to four degenerate singlet states coming from two ^3P states of the carbon atom at the fragment limit. All these four states are bound and are very close in energy along the entire PES. The three states, $1^1\Sigma_g^+$, $1^1\Delta_g$, and $2^1\Sigma_g^+$, which belong to the same space symmetry A_g in a D_{2h} point group also display actual crossings between $^1\Delta_g$ and $^1\Sigma_g^+$ states and an avoided crossing between $1^1\Sigma_g^+$ and $2^1\Sigma_g^+$, making them amenable to Procedure I. Choosing to optimize the lowest state among these three degenerate states ($1^1\Sigma_g^+$, $1^1\Delta_g$, and $2^1\Sigma_g^+$) at dissociation breaks the degeneracy of the three states. A dynamic state average[114] would have been preferred, but as others have shown,[115] there is not much difference in the results if we take an average with equal weights. We have chosen the latter for simplicity. Another state, $1^1\Pi_u$, which belongs to B_{1u} in a D_{2h} point group, also goes to the same fragment limit (^3P + ^3P). The $1^1\Pi_u$ state is the lowest state of its space symmetry and can be thus optimized independently but gives a symmetry broken solution. Since only the active orbitals are explicitly localized using the Pipek−Mezey scheme in preparation of the UGA-SSMRPT2 to follow, the core and virtual orbitals in C_2 remain delocalized although the orbitals are generated in a C_{2v} point group unlike in O_2 where an automatic localization of the core is seen. The core and virtual orbitals on the C atom are perforce localized. The class-diagonality of our H_0 takes care of the rotated core and virtual orbitals, and no reflection of this phenomenon is seen on the size-consistency. However, as expected, with a diagonal H_0, we obtain an SCE of 56 μE_h. As expected, the state averaged energy for the three states ($1^1\Sigma_g^+$, $1^1\Delta_g$, and $2^1\Sigma_g^+$) is slightly higher than the optimized symmetry broken states at the asymptotic limit be it the $1^1\Pi_u$ or the $1^1\Sigma_g^+$ state. The CASSCF energy of these three degenerate states is twice of the carbon atom corresponding to the symmetry restored solution, while the energy of the symmetry broken $1^1\Pi_u$ or $1^1\Sigma_g^+$ is twice of the symmetry broken C atom. The $1^1\Pi_u$ state has been shown to be degenerate with the orbitals of the symmetry restored set of states using the Procedure II.

PES of these four singlet states computed with the UGA-SSMRPT2 method are shown in Figure 5. At the equilibrium region, the $1^1\Sigma_g^+$ state is the ground state. At short distances, the $1^1\Delta_g$ state is the highest in energy among all the states discussed here, but it gradually comes down as the distance increases. First, it crosses the $2^1\Sigma_g^+$ state at 1.2 Å and then the $1^1\Pi_u$ state at 1.5 Å, and after 1.6 Å, it becomes the lowest energy state after crossing the $1^1\Sigma_g^+$ state. The two $^1\Sigma_g^+$ states show an avoided curve crossing at 1.6 Å.

Using delocalized pseudocanonical orbitals in a D_{2h} point group for the MRMP2 method and localized orbitals in a C_{2v} point group for the UGA-SSMRPT2 computation, we have listed the energy differences reflecting their size-consistency in Table 5. MRMP2 shows a size-consistency error of about 0.75 mE_h for the symmetry broken wave function and 3.08 mE_h for the symmetry restored wave function. The UGA-SSMRPT2 is found to be size-consistent below its convergence threshold. CASSCF energy of the symmetry broken wave function of the individual states of the C_2 molecule as well as of the atomic

DOI: 10.1021/acs.jctc.5b00457
J. Chem. Theory Comput. 2015, 11, 4129−4145

Table 5. C_2 Molecule: Size-Consistency Check With cc-pVDZ Basis Set[a]

	C atom	C_2 molecule
	^3P	$X^1\Sigma_g^+$, $B^1\Delta_g$, $B'^1\Sigma_g^+$, $A^1\Pi_u$
	^3P	$^3P + {}^3P$
symmetry broken wave function		
CASSCF	−37.7010866	−75.4021733
SCE		[b]
UGA-SSMRPT2	−37.7446730	−75.4893461
SCE		[b]
MRMP2	−37.7530366	−75.5068285
SCE		$0.7553 mE_h$
symmetry restored wave function		
CASSCF	−37.6997393	−75.3994785
SCE		[b]
UGA-SSMRPT2	−37.7456144	−75.4912289
SCE		[b]
MRMP2	−37.7544005	−75.5118831
SCE		$3.082 mE_h$

[a]Localized orbitals are used for UGA-SSMRPT2 computations. [b]Below convergence threshold ($10^{-2}\mu E_h$).

carbon is lower than the symmetry restored wave function. Interestingly, this energy ordering is reversed on introducing dynamical correlation through the MRMP2 or the UGA-SSMRPT2 method.

SUMMARY AND CONCLUDING REMARKS

We have explored in this paper the various issues which are important in numerically realizing size-consistency, as reflected in the asymptotes of potential energy surfaces (PES), using as a prototype our recently developed UGA-SSMRPT2.[69] It is well known that if a theory is both size-extensive and invariant with respect to transformation within the class of core, active, and virtual orbitals it will be size-consistent. Multireference theories satisfying these two constraints are hard to come by, although the internally contracted multireference coupled cluster(icMRCC) theories[45,47,49]and NEVPT2[60,61] in their most rigorous form belong to this category. These theories, however, come with the burden of high computational cost. For practical applications, the noninvariant theories, which are multireference, intruder-free, and size-extensive, turn out to be cheaper. Prototypical formalisms include the suite of state-specific MRCCs of several varieties,[45,75] their spin-free analogues,[55,76] and the dressed MRCI approach advocated by Malrieu et al.[37,52] These state-specific MRCCs also generate the corresponding perturbative versions sharing the property of size-extensivity. They are thus, deemed by us, as most suitable for studying the PES of large systems. Among the noninvariant perturbative versions originating from the SSMRCC (or MkMRCC) of Mukherjee et al.[44−46] or their spin-free analogues[55,93] are the SSMRPT of Mukherjee et al.[63−66] or their spin-free analogues,[67−69] and we choose the explicitly spin-free UGA-SSMRPT2[69] as a prototype to study size-consistency, using localized orbitals. We have emphasized in the paper that, provided the unperturbed energy shows size-consistency with respect to localized orbitals, size-consistency of the correlated perturbation theories follow as a consequence, at least as a matter of principle. However, the issue of size-consistency of size-extensive orbitally noninvariant state-specific multireference theories, in general, and the perturbation theories (SSMRPTs), in particular, appears to be nontrivial, and we have studied the possible hurdles in the numerical realization of additive separability of energy at the asymptotic limit of PES and suggested possible ways to overcome them. The problems to be resolved to ensure size-consistency of a noninvariant state-specific perturbation theory is, however, generic and is not specific to our UGA-SSMRPT2. Our studies demonstrate, though, the strength of UGA-SSMRPT2 in resolving and analyzing the problems encountered.

We have found that the most commonly encountered problem stems from the zeroth order CASSCF function itself, due to the breaking of degeneracy of orbitals at the asymptotes of PES. The fragment orbitals are then symmetry broken, which leads to consequent distortion of the energetics in the fragmentation limit because of the orbital noninvariance of the perturbation theory. Using a state-averaged CASSCF starting function can restore the symmetry in most cases at the cost of our inability to utilize fully optimized orbitals. We have also suggested an alternative pathway to address this problem, which uses orbitals of a close-lying state going to the same asymptote, if such states are available. We have been able to demonstrate that our UGA-SSMRPT is size-consistent not only when symmetry is restored but also at the symmetry broken asymptote. Of course, in this case, the energies of the fragments will have to be accepted as valid as computed with the broken symmetric fragment orbitals. What is interesting is that in certain situations, the nature of symmetry breaking of the fragments and the corresponding supermolecule turns out to be different. While it is enough to use a "class-diagonal" zeroth order Hamiltonian to ensure size-consistency when the core/virtual orbitals of the fragment and those of the supermolecule are related by an orthogonal transformation, the noninvariance of the correlated theories such as UGA-SSMRPT2 with respect to rotations among active orbitals implies that the rotated active orbitals would lead to loss of size-consistency. We have come across such pathologies in several states of the molecules we have studied.

In the course of our explorations, we were surprised to encounter size-consistent behavior of another commonly used MRPT, the MRMP2 theory, which is generally size-inconsistent. In our paper, we have also presented our analysis of what conditions will lead to this accidental size-consistent behavior for MRMP2.

In conclusion, we emphasize that although our studies have been undertaken on UGA-SSMRPT2, the issues discussed are generic for all orbitally noninvariant state-specific multireference theories, both of the coupled cluster and the perturbative varieties. In fact, some of the issues such as symmetry breaking are also relevant to the CASSCF procedure itself since it leads to erroneous asymptotic energies, although size-consistency is not affected in view of the orbital-invariance of CASSCF.

Since some of the difficulties encountered by us arise from reaching symmetry broken fragment limits at the zeroth order description, viz., the CASSCF level itself, we are looking into the possibility of using softwares where the active orbitals are directly generated as localized.[107,108] This will at least alleviate the pathologies stemming from broken symmetric behavior at the starting point.

AUTHOR INFORMATION

Corresponding Author

*E-mail: pcdm@iacs.res.in.

Notes

The authors declare no competing financial interest.

DOI: 10.1021/acs.jctc.5b00457
J. Chem. Theory Comput. 2015, 11, 4129−4145

■ ACKNOWLEDGMENTS

We thank Mark Gordon for kindly clarifying to us certain aspects of the GAMESS-US program package.[105] We also thank Pradipta Kumar Samanta for discussions at the preliminary stage of our project. A.S. thanks the CSIR and the DST, and S.S. thanks CSIR for financial support. D.M. thanks the SERB for the distinguished fellowship conferred on him. D.M. and S.S. acknowledge the IFCPAR/CEFIPRA for the Indo-French Grant No. 4705-3.

■ DEDICATION

It is a great pleasure for D.M. to dedicate this paper to Andreas Savin, a friend for many years, on the happy occasion of his reaching sixty-five.

■ REFERENCES

(1) Bartlett, R. J.; Purvis, G. D. *Int. J. Quantum Chem.* **1978**, *14*, 561−581.
(2) Bartlett, R. J. *Annu. Rev. Phys. Chem.* **1981**, *32*, 359−401.
(3) Mukherjee, D.; Pal, S. *Adv. Quantum Chem.* **1989**, *20*, 291−373.
(4) Lyakh, D. I.; Musial, M.; Lotrich, V. F.; Bartlett, R. J. *Chem. Rev.* **2012**, *112*, 182−243.
(5) Lyakh, D. I.; Bartlett, R. J. *Mol. Phys.* **2014**, *112*, 213−260.
(6) Pople, J.; Binkley, J.; Seeger, R. *Int. J. Quantum Chem.* **1976**, *10*, 1−19.
(7) Nooijen, M.; Shamasundar, K. R.; Mukherjee, D. *Mol. Phys.* **2005**, *103*, 2277−2298.
(8) Møller, C.; Plesset, M. S. *Phys. Rev.* **1934**, *46*, 618−622.
(9) Pople, J. A.; Krishnan, R.; Schlegel, H. B.; Binkley, J. S. *Int. J. Quantum Chem.* **1978**, *14*, 545−560.
(10) Shavitt, I. In *Methods of Electronic Structure Theory*; Schaefer, H. F., Ed.; Springer US: Boston, MA, 1977; pp 189−275.
(11) Buenker, R. J.; Peyerimhoff, S. D. *Theor. Chim. Acta* **1974**, *35*, 33−58.
(12) Bloch, C. *Nucl. Phys.* **1958**, *6*, 329−347.
(13) Brandow, B. *Rev. Mod. Phys.* **1967**, *39*, 771−828.
(14) Lindgren, I. *J. Phys. B: At. Mol. Phys.* **1974**, *7*, 2441−2470.
(15) Schucan, T. H.; Weidenmüller, H. A. *Ann. Phys.* **1972**, *73*, 108−135.
(16) Schucan, T. H.; Weidenmüller, H. A. *Ann. Phys.* **1973**, *76*, 483−509.
(17) Mukherjee, D.; Moitra, R. K.; Mukhopadhyay, A. *Mol. Phys.* **1977**, *33*, 955−969.
(18) Lindgren, I. *Int. J. Quantum Chem.* **1978**, *14*, 33−58.
(19) Jeziorski, B.; Monkhorst, H. *Phys. Rev. A: At., Mol., Opt. Phys.* **1981**, *24*, 1668−1681.
(20) Ben-Shlomo, S.; Kaldor, U. *J. Chem. Phys.* **1988**, *89*, 956−958.
(21) Kaldor, U. *Chem. Phys.* **1990**, *140*, 1−6.
(22) Kaldor, U. *Theor. Chim. Acta* **1991**, *80*, 427−439.
(23) Ilyabaev, E.; Kaldor, U. *J. Chem. Phys.* **1993**, *98*, 7126−7131.
(24) Sen, S.; Shee, A.; Mukherjee, D. *J. Chem. Phys.* **2012**, *137*, 074104.
(25) Nakano, H. *J. Chem. Phys.* **1993**, *99*, 7983−7992.
(26) Nakano, H. *Chem. Phys. Lett.* **1993**, *207*, 372−378.
(27) Nakano, H.; Nakatani, J.; Hirao, K. *J. Chem. Phys.* **2001**, *114*, 1133−1141.
(28) Hirao, K. *Chem. Phys. Lett.* **1992**, *190*, 374−380.
(29) Hirao, K. *Int. J. Quantum Chem.* **1992**, *44*, 517−526.
(30) Mukherjee, D. *Chem. Phys. Lett.* **1986**, *125*, 207−212.
(31) Mukherjee, D. *Int. J. Quantum Chem.* **1986**, *30*, 409−435.
(32) Mukherjee, D. In *Condensed Matter Theories*; Arponen, J. S., Bishop, R. F., Manninen, M., Eds.; Springer US: Boston, MA, 1988; pp 67−81.
(33) Kaldor, U. In *Condensed Matter Theories*; Arponen, J. S., Bishop, R. F., Manninen, M., Eds.; Springer US: Boston, MA, 1988; Vol. 3; pp 83−92.
(34) Balkova, A.; Kucharski, S. A.; Meissner, L.; Bartlett, R. J. *J. Chem. Phys.* **1991**, *95*, 4311.
(35) Kirtman, B. *J. Chem. Phys.* **1981**, *75*, 798−808.
(36) Malrieu, J. P.; Durand, P.; Daudey, J. P. *J. Phys. A: Math. Gen.* **1985**, *18*, 809−826.
(37) Meller, J.; Malrieu, J. P.; Caballol, R. *J. Chem. Phys.* **1996**, *104*, 4068.
(38) Reguero, M.; Caballol, R.; Heully, J.-l.; Malrieu, J.-p. *Chem. Phys. Lett.* **1997**, *265*, 621−628.
(39) Malrieu, J. P. *Mol. Phys.* **2013**, *111*, 2451−2462.
(40) Pradines, B.; Suaud, N.; Malrieu, J.-P. *J. Phys. Chem. A* **2015**, *119*, 5207−5217.
(41) Mukhopadhyay, D.; Datta (nee Kundu), B.; Mukherjee, D. *Chem. Phys. Lett.* **1992**, *197*, 236−242.
(42) Landau, A.; Eliav, E.; Kaldor, U. *Chem. Phys. Lett.* **1999**, *313*, 399−403.
(43) Musial, M.; Bartlett, R. J. *J. Chem. Phys.* **2011**, *135*, 044121.
(44) Mahapatra, U.; Datta, B.; Mukherjee, D. *Mol. Phys.* **1998**, *94*, 157−171.
(45) Mahapatra, U. S.; Datta, B.; Bandyopadhyay, B.; Mukherjee, D. *Adv. Quantum Chem.* **1998**, *30*, 163−193.
(46) Mahapatra, U. S.; Datta, B.; Mukherjee, D. *J. Chem. Phys.* **1999**, *110*, 6171−6188.
(47) Mukherjee, D. In *Recent Progress in Many Body Theories*, Vol. 4; Mitter, H., Schachinger, E., Sormann, H., Eds.; Plenum Press: New York, 1995; pp 127−133.
(48) Sinha, D.; Maitra, R.; Mukherjee, D. *Comput. Theor. Chem.* **2013**, *1003*, 62−70.
(49) Hanauer, M.; Köhn, A. *J. Chem. Phys.* **2011**, *134*, 204111.
(50) Hanauer, M.; Köhn, A. *J. Chem. Phys.* **2012**, *137*, 131103.
(51) Evangelista, F. a.; Gauss, J. *J. Chem. Phys.* **2011**, *134*, 114102.
(52) Malrieu, J.-P.; Daudey, J.-P.; Caballol, R. *J. Chem. Phys.* **1994**, *101*, 8908−8921.
(53) Hubač, I.; Neogrády, P. *Phys. Rev. A: At., Mol., Opt. Phys.* **1994**, *50*, 4558−4564.
(54) Hubač, I.; Pittner, J.; Čársky, P. *J. Chem. Phys.* **2000**, *112*, 8779−8784.
(55) Maitra, R.; Sinha, D.; Mukherjee, D. *J. Chem. Phys.* **2012**, *137*, 024105.
(56) Roos, B. O.; Andersson, K.; Fülscher, M. P.; Malmqvist, P.-A.; Serrano-Andrés, L.; Pierloot, K.; Merchán, M. In *Advances in Chemical Physics: New Methods in Computational Quantum Mechanics*; Prigogine, I., Rice, S., Eds.; John Wiley & Sons, Inc., 1996; Vol. 93; pp 219−331.
(57) Andersson, K.; Malmqvist, P.; Roos, B. O.; Sadlej, A. J.; Wolinski, K. *J. Phys. Chem.* **1990**, *94*, 5483−5488.
(58) van Dam, H. J. J.; van Lenthe, J. H.; Pulay, P. *Mol. Phys.* **1998**, *93*, 431−439.
(59) Celani, P.; Werner, H. J. *J. Chem. Phys.* **2000**, *112*, 5546−5557.
(60) Angeli, C.; Cimiraglia, R.; Evangelisti, S.; Leininger, T.; Malrieu, J. P. *J. Chem. Phys.* **2001**, *114*, 10252−10264.
(61) Angeli, C.; Cimiraglia, R. *J. Phys. Chem. A* **2014**, *118*, 6435−6439.
(62) (a) Witek, H. A.; Nakano, H.; Hirao, K. *J. Chem. Phys.* **2003**, *118* (18), 8197−8206. (b) Witek, H. A.; Nakano, H.; Hirao, K. *J. Comput. Chem.* **2003**, *24* (12), 1390−1400.
(63) Mahapatra, U. S.; Datta, B.; Mukherjee, D. *Chem. Phys. Lett.* **1999**, *299*, 42−50.
(64) Mahapatra, U. S.; Datta, B.; Mukherjee, D. *J. Phys. Chem. A* **1999**, *103*, 1822−1830.
(65) Ghosh, P.; Chattopadhyay, S.; Jana, D.; Mukherjee, D. *Int. J. Mol. Sci.* **2002**, *3*, 733−754.
(66) Evangelista, F. A.; Simmonett, A. C.; Schaefer, H. F., III; Mukherjee, D.; Allen, W. D. *Phys. Chem. Chem. Phys.* **2009**, *11*, 4728−4741.
(67) Mao, S.; Cheng, L.; Liu, W.; Mukherjee, D. *J. Chem. Phys.* **2012**, *136*, 024105.
(68) Mao, S.; Cheng, L.; Liu, W.; Mukherjee, D. *J. Chem. Phys.* **2012**, *136*, 024106.

DOI: 10.1021/acs.jctc.5b00457
J. Chem. Theory Comput. 2015, 11, 4129−4145

(69) Sen, A.; Sen, S.; Samanta, P. K.; Mukherjee, D. *J. Comput. Chem.* **2015**, *36*, 670−688.
(70) Nooijen, M.; Lotrich, V. J. *J. Chem. Phys.* **2000**, *113*, 494−507.
(71) Kong, L.; Shamasundar, K. R.; Demel, O.; Nooijen, M. *J. Chem. Phys.* **2009**, *130*, 114101.
(72) Datta, D.; Kong, L.; Nooijen, M. *J. Chem. Phys.* **2011**, *134*, 214116.
(73) Datta, D.; Nooijen, M. *J. Chem. Phys.* **2012**, *137*, 204107.
(74) Nooijen, M.; Demel, O.; Datta, D.; Kong, L.; Shamasundar, K. R.; Lotrich, V.; Huntington, L. M.; Neese, F. J. *J. Chem. Phys.* **2014**, *140*, 081102.
(75) Das, S.; Pathak, S.; Datta, D.; Mukherjee, D. *J. Chem. Phys.* **2012**, *136*, 164104.
(76) Sinha, D.; Maitra, R.; Mukherjee, D. *J. Chem. Phys.* **2012**, *137*, 094104.
(77) Hoffmann, M. R.; Datta, D.; Das, S.; Mukherjee, D.; Szabados, A.; Rolik, Z.; Surján, P. R. *J. Chem. Phys.* **2009**, *131*, 204104.
(78) Angeli, C.; Cimiraglia, R.; Malrieu, J.-P. *Chem. Phys. Lett.* **2000**, *317*, 472−480.
(79) Hoffmann, M. R. *J. Phys. Chem.* **1996**, *100*, 6125−6130.
(80) Khait, Y. G.; Song, J.; Hoffmann, M. R. *J. Chem. Phys.* **2002**, *117*, 4133−4145.
(81) Jiang, W.; Khait, Y. G.; Hoffmann, M. R. *J. Phys. Chem. A* **2009**, *113*, 4374−4380.
(82) Rolik, Z.; Szabados, A.; Surján, P. R. *J. Chem. Phys.* **2003**, *119*, 1922−1928.
(83) Szabados, A.; Surján, P. R. In *Fundamental World of Quantum Chemistry, A Tribute to the Memory of Per-Olov Lowdin*; Brändas, E. J., Kryachko, E. S., Kluwer, D., Eds.; Springer, 2004; Vol. *III*; pp 129−185.
(84) Szabados, A.; Rolik, Z.; Tóth, G.; Surján, P. R. *J. Chem. Phys.* **2005**, *122*, 114104.
(85) Rosta, E.; Surján, P. R. *J. Chem. Phys.* **2002**, *116*, 878−890.
(86) Jeszenszki, P.; Nagy, P. R.; Zoboki, T.; Szabados, A.; Surján, P. R. *Int. J. Quantum Chem.* **2014**, *114*, 1048−1052.
(87) Xu, E.; Li, S. *J. Chem. Phys.* **2013**, *139*, 174111.
(88) Liu, W.; Hoffmann, M. R. *Theor. Chem. Acc.* **2014**, *133*, 1481.
(89) Roos, B.; Lawley, K. In *Advances in Chemical Physics: Ab Initio Methods in Quantum Chemistry II*; Lawley, K. P., Ed.; John Wiley & Sons, Inc., 1987; Vol. *69*; pp 399−446.
(90) Čársky, P.; Pittner, J.; Hubač, I. In *Theory and Applications of Computational Chemistry: The First Forty Years*; Dykstra, C. E., Frenking, G., Kim, K. S., Scuseria, G. E., Eds.; Elsevier B.V, 2005; pp 465−481.
(91) Bartlett, R. J.; Musial, M. *Rev. Mod. Phys.* **2007**, *79*, 291−352.
(92) Köhn, A.; Hanauer, M.; Mück, L. A.; Jagau, T.-C.; Gauss, J. *WIRE: Comp. Mol. Sci.* **2013**, *3*, 176−197.
(93) Maitra, R.; Sinha, D.; Sen, S.; Shee, A.; Mukherjee, D. *Theory and Applications in Computational Chemistry: The First Decade of the Second Millennium: International Congress TACC-2012*; AIP Publishing, 2012; Vol. *1456*, pp 81−96.
(94) Sayós, R.; Valero, R.; Anglada, J. M.; González, M. *J. Chem. Phys.* **2000**, *112* (15), 6608−6624.
(95) Zaitsevskii, A.; Malrieu, J. P. *Chem. Phys. Lett.* **1996**, *250*, 366−372.
(96) Li, X.; Paldus, J. *J. Chem. Phys.* **1994**, *101*, 8812−8826.
(97) Janssen, C. L.; Schaefer, H. F. *Theor. Chim. Acta* **1991**, *79*, 1−42.
(98) Evangelista, F. A.; Allen, W. D.; Schaefer, H. F. *J. Chem. Phys.* **2007**, *127*, 024102.
(99) Maitra, R.; Sinha, D.; Sen, S.; Mukherjee, D. *Theor. Chem. Acc.* **2014**, *133*, 1522.
(100) Jeszenszki, P.; Surján, P. R.; Szabados, A. *J. Chem. Phys.* **2013**, *138*, 124110.
(101) Heully, J. L.; Malrieu, J. P.; Zaitsevskii, A. *J. Chem. Phys.* **1996**, *105*, 6887−6891.
(102) Das, S.; Datta, D.; Maitra, R.; Mukherjee, D. *Chem. Phys.* **2008**, *349*, 115−120.
(103) Rintelman, J. M.; Adamovic, I.; Varganov, S.; Gordon, M. S. *J. Chem. Phys.* **2005**, *122*, 044105.
(104) Potts, D. M.; Taylor, C. M.; Chaudhuri, R. K.; Freed, K. F. *J. Chem. Phys.* **2001**, *114*, 2592−2600.
(105) Schmidt, M. W.; Baldridge, K. K.; Boatz, J. A.; Elbert, S. T.; Gordon, M. S.; Jensen, J. H.; Koseki, S.; Matsunaga, N.; Nguyen, K. A.; Su, S.; Windus, T. L.; Dupuis, M.; Montgomery, J. A. *J. Comput. Chem.* **1993**, *14*, 1347−1363.
(106) Dyall, K. G. *J. Chem. Phys.* **1995**, *102*, 4909−4918.
(107) Maynau, D.; Evangelisti, S.; Guihéry, N.; Calzado, C. J.; Malrieu, J.-P. *J. Chem. Phys.* **2002**, *116*, 10060.
(108) Angeli, C.; Evangelisti, S.; Cimiraglia, R.; Maynau, D. *J. Chem. Phys.* **2002**, *117*, 10525−10533.
(109) Chattopadhyay, S.; Mahapatra, U. S.; Chaudhuri, R. K. *J. Phys. Chem. A* **2009**, *113*, 5972−5984.
(110) Mahapatra, U. S.; Chattopadhyay, S.; Chaudhuri, R. K. *J. Chem. Phys.* **2008**, *129*, 024108.
(111) Mahapatra, U. S.; Chattopadhyay, S.; Chaudhuri, R. K. *J. Chem. Phys.* **2009**, *130*, 014101.
(112) Pipek, J.; Mezey, P. G. *J. Chem. Phys.* **1989**, *90*, 4916−4926.
(113) Su, P.; Wu, J.; Gu, J.; Wu, W.; Shaik, S.; Hiberty, P. C. *J. Chem. Theory Comput.* **2011**, *7*, 121−130.
(114) Deskevich, M. P.; Nesbitt, D. J.; Werner, H.-J. *J. Chem. Phys.* **2004**, *120*, 7281−7289.
(115) Zeng, T.; Fedorov, D.; Klobukowski, M. *J. Chem. Phys.* **2011**, *134*, 024108.

DOI: 10.1021/acs.jctc.5b00457
J. Chem. Theory Comput. 2015, 11, 4129−4145